A Major Project Report on

"DESIGN OF ADVANCED UAV LANDING SYSTEM USING QUANTUM LOCKING MECHANISM"

Submitted in partial fulfilment of the requirement for the award of degree of

BACHELOR OF TECHNOLOGY

in

AERONAUTICAL ENGINEERING

by

KASARLLA PRANATHI	**20R21A2124**
NUKALA MANISHANKAR	**20R21A2140**
ROHAN SAI ADISERLA	**20R21A2145**

Under the esteemed guidance of

Mr. K Veeranjaneyulu (PhD), M.E

Professor

Department of Aeronautical Engineering

at

MARRI LAXMAN REDDY GROUP OF INSTITUTIONS

MLR Institute of Technology

(Approved by AICTE and Permanent Affiliated to JNTU, Hyderabad)

(UGC-Autonomous)

Laxman Reddy Avenue, Dundigal, Quthbullapur Mandal, Hyderabad-43. R.R.Dist.

2020-24

Affiliated to

Jawaharlal Nehru Technological University

Kukatpally, Hyderabad

2024

MLR Institute of Technology

(Approved by AICTE and Affiliated to JNTU, Hyderabad)

Laxman Reddy Avenue, Dundigal, Qutbullapur Mandal, Hyderabad-43. R.R.Dist.

2020-24

CERTIFICATE

This is to certify that the Major Project report entitled **"DESIGN OF ADVANCED UAV LANDING SYSTEM USING QUANTUM LOCKING MECHANISM"** is the Bonafide work carried out and submitted by

KASARLLA PRANATHI	**20R21A2124**
NUKALA MANISHANKAR	**20R21A2140**
ROHAN SAI ADISERLA	**20R21A2145**

To the Department of Aeronautical Engineering, MLR Institute of Technology Hyderabad, In partial fulfilment for the award of **BACHELOR OF TECHNOLOGY IN AERONAUTICAL ENGINEERING** during the academic year 2023-2024.

Internal Guide

Mr. K Veeranjaneyulu (PhD), M.E

Professor

Department of Aeronautical Engineering

Head of Department

Dr. Satyanarayana Gupta PhD, M.Tech,

Professor & Head

Department of Aeronautical Engineering

External Examiner

ACKNOWLEDGEMENT

The satisfaction and euphoria that accompany the successful completion of any task would be incomplete without the mention of people who made it possible, whose constant guidance and encouragement crowned our efforts with success. It is a pleasant aspect that we now have the opportunity to express our guidance for all of them. We are thankful to **Mr. M Raja Shekar Reddy ‘**Secretary of MLR Institute of Technology**’** for giving us an opportunity to do a project in their esteemed organization.

We are thankful to our Principal **Dr. Srinivas Rao** MTech, PhD, MISTE, MIE of ‘MLR Institute of Technology’ for helping us to achieve a successful project as a part of university curriculum.

Our special thanks to **Dr. M Satyanarayana Gupta** MTech, PhD Professor & Head in Aeronautical Department and **Mr. K Veeranjaneyulu** M.E, (PhD), Professor in Aeronautical Department for guiding us in the right way to complete our project in the right time. We would like to thank our internal project mates and department professors for their full-fledged guidance and giving courage to carry out the project.

We are thankful to everyone who helped us for the successful completion of our project.

KASARLLA PRANATHI 20R21A2124
NUKALA MANISHANKAR 20R21A2140
ROHAN SAI ADISERLA 20R21A2145

DECLARATION

We do declare that the project work entitled **"DESIGN OF ADVANCED UAV LANDING SYSTEM USING QUANTUM LOCKING MECHANISM"** submitted in the department of Aeronautical Engineering (AE), **MLR Institute of Technology**, Hyderabad-43, in partial fulfilment of the requirement for the award of the degree of **Bachelors of Technology in AERONAUTICAL ENGINEERING** is a Bonafide record of our own work carried out at **MLRIT** under the esteemed supervision of **Mr. K Veeranjaneyulu** M.E, (PhD), Professor in Aeronautical Department, MLR Institute of Technology.

Also, we declare that the matter embodied in this major project has not been submitted previously by anyone to any other university or institute for the award of any other degree/diploma.

KASARLLA PRANATHI **20R21A2124**
NUKALA MANISHANKAR **20R21A2140**
ROHAN SAI ADISERLA **20R21A2145**

ABSTRACT

In recent years, the utilization of Unmanned Aerial Vehicles (UAVs) has surged across diverse sectors such as military operations, agriculture, surveillance, and logistics. This expansion has underscored the critical need for innovative landing systems capable of ensuring precise and reliable landings under various conditions. Traditional GPS-based systems, while widely used, face limitations in accuracy and susceptibility to interference. To address these challenges, emerging technologies like quantum levitation have emerged as promising solutions, offering unprecedented precision and reliability in UAV landings.

Introducing the groundbreaking concept of the UAV Landing System Using Quantum Locking Mechanism, this project leverages the principles of superconductivity to revolutionize UAV landing capabilities. Quantum locking presents a transformative approach to overcome the shortcomings of conventional methods, promising enhanced precision and reliability. The project delves into the fundamental principles of quantum locking and its integration with UAV landing systems, highlighting its advantages over traditional techniques. Furthermore, it identifies ideal materials and designs for this innovative landing mechanism.

TABLE OF CONTENT

CONTENTS:

LIST OF FIGURES:

LIST OF TABLES:

CHAPTER 1: INTRODUCTION

1.1: Introduction

As societies around the world are heading towards development, with cities becoming more congested, our current ways of transportation will no longer be able to sustain such packed areas. India, being the country with the largest railroad network in the world, uses conventional rails for transporting passengers as well as freight. Other countries such as 1 Morocco have developed high-speed rail systems, connecting major cities throughout the country. Sadly, these transportation systems have become obsolete due to its many 2 challenges. The limitations of the aforementioned transportation systems include limitation of land, their impact on the global environment, and most importantly the misuse of energy in the vehicle. There is a lack of efficiency, disabling the transportation system to exhibit its full potential performance. Due to the presence of friction between the wheels and the ground, there is a rolling resistance causing some energy to be wasted into thermal energy rather than kinetic energy. If the wasted energy is redirected into kinetic energy, future transportation systems can become more efficient, allowing the vehicle to operate at a much greater speed with less energy consumed.

The solution to this problem lies in the development of future transportation systems through the use of electromagnets and superconducting magnets. The use of electromagnets will allow engineers to develop magnetic levitating trains, which will have no physical contact with the ground. Ergo, the amount of friction between the train and the ground will reduce substantially. The reduction of friction allows more energy to be conserved and used as kinetic energy rather than wasted into thermal energy. The idea of using electromagnets in transportation systems is already existing and known as the ‘MagLev Train’. To this date, there are two types of magnetically levitated trains that are in service:

Electromagnetic Suspension (EMS) - Electromagnetic suspension (EMS) uses the attractive force between magnets present on the train’s sides and underside and on he guideway to levitate the train.

Electrodynamic Suspension (EDS) - Electrodynamic suspension (EDS) systems are similar to EMS in several respects, but the magnets are used to repel the train from the guideway rather than attract them.

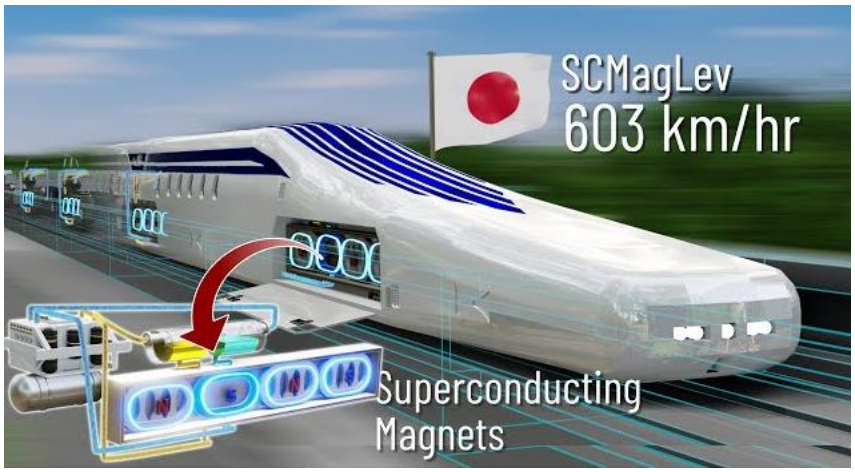

Fig 1.1: Maglev train levitation

1.2: Historical Review

Automatic Landing System (ALS):

The Automatic Landing System (ALS) represents a cutting-edge advancement in UAV technology, employing a sophisticated integration of state-of-the-art sensors, including radar and lidar, and guidance systems to enable fully automated landing procedures. This system is designed with precision control mechanisms, significantly reducing the reliance on human intervention during the critical phase of landing. Originally developed for military applications, ALS has found widespread use in diverse sectors, including commercial drone operations, where precise and repeatable landings are paramount.

Advanced Sensor Integration: ALS incorporates sophisticated sensors, including radar and lidar, combined with guidance systems to enable fully automated UAV landings.

Precision Control: Designed for precise control during the landing phase, reducing the need for human intervention.

Versatility: Applicable in various scenarios, from military applications to commercial drone operations.

Table 1.1: Advantages and Disadvantages of ALS

ADVANTAGES	DISADVANTAGES
– High Precision – Reduced Human Intervention – Adaptability – Enhanced Safety	– Cost – Complexity – Environmental Sensitivity

GPS-based Landing System:

The GPS-based Landing System stands as a testament to the marriage of satellite technology and unmanned aerial vehicles (UAVs), utilizing signals from global positioning system (GPS) satellites to guide UAVs to predetermined landing locations. This system is characterized by its widespread applicability, providing global coverage for UAV operations. Its straightforward implementation and compatibility with various UAV platforms equipped with GPS receivers have contributed to its popularity in a diverse range of environments.

Satellite Guidance: Utilizes signals from global positioning system (GPS) satellites to guide UAVs to specific landing locations.

Widespread Applicability: Suited for various environments, providing global coverage for UAV operations.

Ease of Implementation: Generally simpler to implement compared to more complex landing systems.

Table 1.2: Advantages and Disadvantages of GPS LS

ADVANTAGES	DISADVANTAGES
– Global Positioning Accuracy – Versatility – Ease of Implementation – Cost-Effective	– Limited Precision in Complex Environments – Vulnerability to GPS Jamming – Dependence on Satellite Signals – Altitude Limitations

Visual Landing Aid (VLA):

The Visual Landing Aid (VLA) system represents a fusion of simplicity and effectiveness in guiding unmanned aerial vehicles (UAVs) during the crucial landing phase. This system relies on visual cues, often in the form of markers or references, to provide guidance to UAVs as they approach the landing site. VLA is frequently employed in conjunction with other landing systems, enhancing precision and adaptability in various operational scenarios. Its adaptability makes it suitable for environments where visual references are available, offering an additional layer of guidance.

Visual Cues: Involves the use of visual markers or cues to guide UAVs during the landing phase.

Complementary System: Often used in conjunction with other landing systems for added precision.

Adaptability: Suitable for scenarios where visual references are available.

Table 1.3: Advantages and Disadvantages of VLA

ADVANTAGES	DISADVANTAGES
– Adaptability – Backup System – Cost-Effective	– Visibility Dependency – Obstruction Sensitivity – Limited Precision

Wire Arresting System:

The Wire Arresting System, inspired by the technology employed on aircraft carriers, represents a unique approach to unmanned aerial vehicle (UAV) landings. This system utilizes cables on the ground to catch and decelerate UAVs upon landing. Designed with the intention of minimizing landing distances, it is particularly well-suited for applications where space is constrained. This technology draws from the proven principles of cable-based landing systems used in naval aviation.

Cable-based Deceleration: Utilizes cables on the ground to catch and decelerate UAVs upon landing.

Aircraft Carrier Inspiration: Draws inspiration from the cable-based landing systems used on aircraft carriers.

Short Landing Distances: Designed to enable shorter landing distances, crucial for confined spaces.

Table 1.4: Advantages and Disadvantages of WAS

ADVANTAGES	DISADVANTAGES
– Short Landing Distances – Mimics Aircraft Carrier Technology – Reduced Runway Requirements – Safety Benefits	– Calibration Challenges – Maintenance Intensive – Infrastructure Requirements

Parachute Recovery System:

The Parachute Recovery System represents a safety-focused solution for unmanned aerial vehicles (UAVs), introducing a reliable mechanism for controlled descents and emergency recoveries. This system is designed to deploy parachutes to slow down and guide UAVs safely to the ground, particularly in situations where traditional landing methods may be compromised. The emphasis on safety and protection of both the UAV and its payload makes the Parachute Recovery System a valuable addition to the toolkit of UAV operators.

Parachute Deployment: Involves deploying parachutes to slow down and guide UAVs for a controlled descent.

Emergency Recovery: Primarily used for emergency recovery in case of system failures or unexpected events.

Safety Emphasis: Prioritizes safety by providing a reliable recovery mechanism.

Table 1.5: Advantages and Disadvantages of PRS

ADVANTAGES	DISADVANTAGES
– Emergency Recovery – Versatility – Rapid Deployment – Payload Protection	– Imprecise Landings – Limited Reusability – Altitude Requirements

Net Capture System:

The Net Capture System is an innovative and dynamic solution in the realm of unmanned aerial vehicle (UAV) recovery. This system employs nets, either deployed from the ground or another vehicle, to capture UAVs during their descent or even in mid-air. The Net Capture System is designed to offer a precise and adaptable method for recovering UAVs, especially in scenarios where traditional ground-based landings are impractical or challenging. This technology has found applications in various fields, ranging from military operations to scientific research and commercial drone deployments.

Mid-air Capture: Uses nets to capture UAVs either in mid-air or during the descent.

Precision Capture: Designed for precise capture of UAVs in motion, providing a unique recovery method.

Adaptability: Suitable for challenging environments where traditional landings are impractical.

Table 1.6: Advantages and Disadvantages of NCS

ADVANTAGES	DISADVANTAGES
– Mid-air Capture Capability – Confined Space Applicability – Low Impact – Adaptability	– Precise Coordination Required – Risk to UAV – Complex Mechanism

1.3: What is magnetism?

Magnetism is a quantum phenomenon whose effects are observed on a macroscopic scale. At the level of the atom, each electron has a small magnetic moment. Naturally, electrons of opposite magnetic moments tend to cluster in pairs. At the atomic level, the magnetization is equal to zero. However, if the electrons find themselves without partners, their magnetic moments add up. Transition metals and rare earth materials are the only elements to carry such a magnetic moment. According to Georgia State University's Hyper Physics website, a magnetic field applies force on electrons in the field because of the Lorentz Force. Lorentz force, or electromagnetic force, is the force experienced by a charged particle in an electromagnetic field. This is the main manifestation of the electromagnetic interaction. It can be further explained with the equation below:

$$\vec{F} = q \times (\vec{E} + \vec{v} \wedge \vec{B})$$

Where q represents the charge of the particle (positive or negative) on which is exerted, force, corresponds to its speed, B and E , respectively, the electric field and the magnetic field. The symbol Λ corresponds to the vector product. Hence, the force applied on an electrically charged particle relies on the strength of the magnetic field, the magnitude of the charge, and the velocity of the particle.

1.4: Types of magnetism

All materials have different magnetic behavior. The factor altering each material's behavior to magnets depends on the core structure of atoms and the temperature it is exposed to. The electron configuration may cause a decrease of magnetism in the material by aligning the magnetic moments in a manner that would cancel each other out. On the other hand, the electron configuration may also cause an increase of magnetic behavior in the material by aligning the magnetic moments. Another factor altering the magnetism behavior in the material is temperature. The increase of temperature results in increased random thermal motion, therefore, complicating the alignments of electrons, hence, the magnetic strength decreases.

There are several types of magnetism, categorizing each material into a category by identifying their magnetic behavior with the factors aforementioned.

Paramagnetism:

Paramagnetism is a type of attraction whereby certain materials are pulled in by a remotely applied attractive field and form an internal induced magnetic field in the direction of the applied magnetic fields.

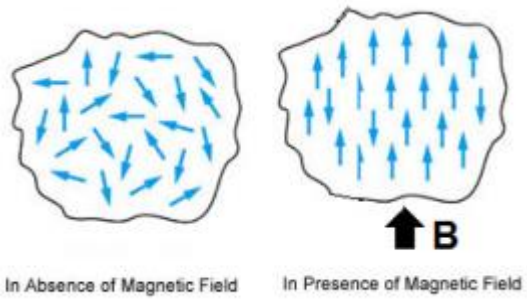

Fig 1.2: Paramagnetism

Ferromagnetism:

Ferromagnetic materials can assemble permanent magnets and are attracted to other magnets. The magnetic moments of the ferromagnet's electrons tend to remain aligned even in the absence of a magnetic field.

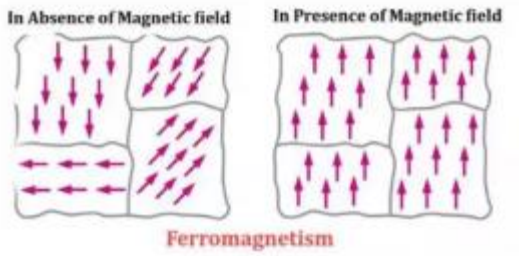

Fig 1.3: Ferromagnetism

Diamagnetism:

Diamagnetism is a kind of magnetism characteristic of materials that line up at right angles to a nonuniform magnetic field and that partly expel from their interior the magnetic field in which they are placed.

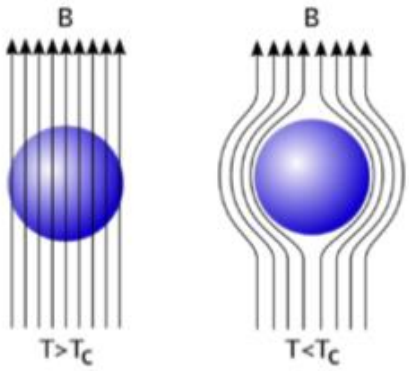

Fig 1.4: Diamagnetism

1.5: Quantum Levitation

Quantum levitation, or quantum locking, is the process in which superconductors uses to levitate over a magnetic source. The effect of quantum levitation occurs because of two 8 natural phenomena: the Meissner effect and flux pinning.

Meissner Effect:

"When Superconductors, are cooled below the critical temperature, they expel magnetic fields and do not allow the magnetic field to penetrate inside them. This phenomenon in superconductors is called the Meissner effect" (Electrical4U, 2019). It does 9 this by covering the surface of the superconductor with small currents, neglecting all of the magnetic fields approaching the superconductor.

This natural phenomenon was manifested by German physicists Walther Meissner and Robert Ochsenfeld in 1933. 9 The two physicists discovered the Meissner effect when exploring the magnetic field intensity around certain materials; they then found that when the materials became superconducting, the magnetic field intensity, dropped close to zero.

Through observations the two physicists concluded that superconductors allow electrons to flow with zero resistance. Due to zero resistivity, small currents are created and rests along the surface of the superconductor, canceling out the magnetic fields approaching the material.

Flux Pinning:

Flux pinning is a quantum phenomenon in which the magnetic flux becomes locked within the superconductor. It is achieved from non-superconducting inclusions and impurities of the crystalline structure from the superconductor. Previously mentioned, due to the Meissner effect small currents along the surface of the superconductor neglects all magnetic flux causing it to go around the material. However, due to some imperfection of the crystalline structure of the superconductor, the pinning is able to slip through the material because of the existence of flux tubes.

One of the key elements for the quantum levitation process are flux tubes. Flux tubes, otherwise known as flux vortices, usually form with type-II superconductors or type-I superconductors that have a thickness of 1-3 microns. With these attributes, less energy is required for the magnetic flux to penetrate through the superconductor.

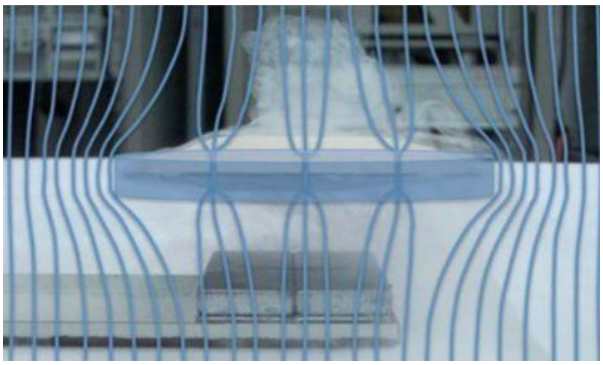

Fig 1.5: Flux Pinning

1.6: Objective

Demonstrate stable levitation and control of UAV prototype over conductor surface using quantum locking phenomena

- Design optimized superconducting magnet assemblies and control mechanisms for integration into UAV airframe.
- Develop cryogenic systems to achieve superconducting conditions for quantum locking landing gear.
- Test and validate precision landing capability.

- Develop modular quantum locking platforms for rapid deployment in uneven terrain or on naval platforms.
- Refine overall UAV and landing platform design for reduced size, weight and power consumption.
- Carry out test flights to 100 cycles to verify endurance and consistency of quantum locking landing systems.
- Demonstrate advantages in landing precision, stability, and environ-mental robustness over state-of-the-art conventional UAV landing approaches

1.7: Motivation

Quantum locking landing gear is expected to have significant advantages over conventional wheel or skid-based systems:

- Greatly improved landing precision: Quantum locking allows the UAV to stably hover centimeters above the landing platform during final descent and touchdown. This enables precision positioning for smooth landing even in tight or obstructed landing zones, overcoming limitations of conventional landing gears.
- All-weather operability: Quantum locking is inherently resistant to conditions like rain, snow and high winds that can destabilize and damage conventional landing gears. This ensures reliable landing capability in harsh environments.
- Simplified, lightweight mechanics: Quantum locked landing gear eliminates the need for complex components like shock absorbers, hydraulics, control surfaces and braking systems required in conventional designs. This reduces weight, simplifies maintenance and improves ruggedness.
- Low-impact touchdown: Magnetic levitation enables soft, controlled touchdown without any hard impact or jolt. This prevents structural damage to the UAV upon landing.
- Rapid redeployment: With no mechanical constraints or interfaces with ground, quantum-locked UAVs can takeoff again in minutes. Conventional landing gears require longer preparation for redeployment.

- Versatility: The quantum locking platform is compact and passive. This enables deployment in space-constrained zones like ships or urban areas, expanding operational capability.
- Future-proofing: Quantum locking technology is still emerging and offers scope for improvements in payload capacity, power and costs. Investing now allows exploiting these future advances.

In summary, this novel landing technology is expected to deliver transformative capabilities unattainable through conventional approaches. It promises to greatly expand the reliability, precision and efficiency of UAV operations across diverse civilian and military applications.

CHAPTER 2: LITERATURE SURVEY

High temperature superconducting magnetic levitation applications - Moon (2004) [1]

The paper offers a comprehensive review of the principles and applications of high-temperature superconducting (HTS) magnetic levitation. The focus is on elucidating fundamental concepts such as flux pinning, hard superconductors, and the Meissner effect, which contribute to stable levitation using HTS materials. The authors delve into various application areas, demonstrating the versatility of HTS levitation across different fields.

Key Findings:

- Fundamental Concepts: The paper discusses crucial principles like flux pinning, hard superconductors, and the Meissner effect. These concepts are essential for understanding how stable levitation is achieved using HTS materials.
- Application Areas: The authors survey key application areas where HTS magnetic levitation finds use. This includes maglev transportation, flywheels for energy storage, magnetic bearings, momentum wheels, linear motors, and vibration isolation. This suggests that HTS levitation has diverse applications in transportation, energy storage, and industrial settings.
- Advantages Over Conventional Methods: The paper highlights the advantages of using HTS materials over conventional superconductors and electromagnets in magnetic levitation systems. This may include improved performance, energy efficiency, or other desirable characteristics.
- Feasibility of Large-Scale HTS Levitation Systems: The paper validates the feasibility of implementing large-scale HTS levitation systems. This suggests that the technology is not merely theoretical but can be practically applied on a significant scale.
- Direction for Further Research: The overview likely provides insights into areas where further research is needed. This may include optimizing HTS

design, refining levitation control methods, and exploring additional applications, such as in maglev trains.

Conclusion:

In summary, the paper serves as a comprehensive overview of HTS magnetic levitation, emphasizing its principles, applications, advantages, and feasibility for large-scale systems. The information provided is expected to contribute to the understanding of HTS technology and guide future research in areas such as design optimization, control mechanisms, and broader applications in transportation and industry.

A research review on magnetic Levitation trains [2]

This paper involves the design, hardware, technology, application and future uses of "Magnetic levitation trains." The maglev transportation system is more stable, faster, economic, efficient. Maglev systems are currently in use for applications such as bearings, high- speed trains, and manufacturing. Maglev is a method of propulsion that uses magnetic levitation to propel vehicles with magnets rather than with wheels, axles and bearings. With maglev, a vehicle is levitated a short distance away from a guide way using magnets to create both lift and thrust (levitation would not exceed above 10 centimeters). In future these High-speed maglev trains would give a huge competition to the aviation industry.

Key Findings:

- Maglev Advantages: The maglev transportation system offers increased stability compared to traditional modes of transportation. Higher speed is achieved through maglev systems, contributing to more efficient and rapid travel. Maglev systems demonstrate economic efficiency, potentially making them a competitive option in certain applications.
- Current Applications: Maglev technology is currently utilized in various applications, including bearings and high-speed trains. The absence of wheels, axles, and bearings in maglev systems contributes to improved performance and smoother operation.

- Maglev Propulsion Method: The paper emphasizes the magnetic levitation method in maglev propulsion, relying on magnets to create lift and thrust. The levitation distance is highlighted as a short distance from the guide way, not exceeding 10 centimeters.

Conclusion:

In conclusion, the paper provides a comprehensive exploration of magnetic levitation trains, revealing several key findings. Maglev systems offer notable advantages in terms of stability, speed, and economic efficiency. Current applications in bearings and high-speed trains demonstrate the practicality and effectiveness of maglev technology. The magnetic levitation propulsion method, which eliminates the need for traditional components like wheels and axles, is a crucial aspect of the maglev system's success. The paper acknowledges the short levitation distance from the guide way, underscoring the precision and control involved in maglev transportation.

Quantum Levitation — Flying vehicles in the near future? [3]

This project aims to study the properties of quantum levitation and locking and provide ways to improve the efficiency and speed of current transportation systems (high-speed trains, levitating cars, and hoverboards), and the idea of creating bearings with negligible friction. This experiment will be approached by placing a Yttrium Barium Copper Oxide (YBCO) superconductor on a Ø40cm Maglev track. Further observations can be made with a Handheld magnetic device to observe the Meissner Effect and explain the physics of the quantum phenomenon.

Key Findings:

- Quantum Levitation and Locking: The experiment successfully demonstrates quantum levitation and locking using a Yttrium Barium Copper Oxide (YBCO) superconductor on a Maglev track. Observations with a handheld magnetic device confirm the presence of the Meissner Effect, providing a visual representation of the quantum phenomenon.
- Efficiency and Speed Improvement: Quantum levitation and locking show promise for enhancing the efficiency and speed of transportation systems. The

application of quantum principles to high-speed trains, levitating cars, and hoverboards could lead to significant improvements in performance and energy efficiency.

- Frictionless Bearings: The experiment supports the idea of creating bearings with negligible friction using quantum levitation. This has the potential to revolutionize various industries, particularly in transportation, by minimizing energy losses due to friction.

- High-Temperature Superconductors (YBCO): The choice of Yttrium Barium Copper Oxide (YBCO) as the superconductor is validated, indicating its effectiveness in achieving high-temperature superconductivity and enabling practical applications of quantum levitation.

Conclusion:

In conclusion, the project successfully explores the properties of quantum levitation and locking, showcasing their potential applications in transportation systems. The Meissner Effect observation provides a tangible understanding of the underlying physics. The demonstrated efficiency and speed improvements through quantum levitation suggest a transformative impact on high-speed trains, levitating cars, and hoverboards. The concept of creating bearings with negligible friction aligns with the project's goals and opens avenues for innovation in multiple industries. The use of YBCO as a high-temperature superconductor underscores its suitability for practical applications of quantum levitation. This project lays the groundwork for further research and development in the field of quantum transportation, paving the way for advancements in speed, efficiency, and frictionless motion.

Quantum Locking and the Meissner Effect Lead to the Origin and Stability of the Saturn Rings System [4]

It is demonstrated how superconducting iced particles of the protoplanetary cloud of Saturn are coming to magnetic equator plane and create the stable enough rings disk. There are two steps. First, after appearance of the Saturn magnetic field due to Meissner phenomenon, all particles' orbits are moving to the magnetic equator

plane. Finally, they become distributed as rings and gaps like iron particles around magnet on laboratory table. And they are separated from each other by the magnetic field expelled from them. It takes up to few tens of thousands years with ten meters rings disk thickness. Second, because of quantum locking all particles become to be locked within magnetic well at the magnetic equator plane due to Abrikosov vortex for superconductor. Finally, each particle is locked within three-dimensional magnetic well. It works even when particles have small fraction of superconductor. During the rings evolution some contribution to the disk also could come from the collision-generated debris of the current moon, coming meteorites and from the geysers like it happened due to magnetic coupling of Saturn and Enceladus. The rings are relict of the early days of the magnetic field of Saturn system.

Key Findings:

- Meissner Phenomenon and Alignment: As Saturn's magnetic field appears, a Meissner phenomenon occurs, causing all particles within the protoplanetary cloud to align along the magnetic equator plane. Over time, these particles become distributed as rings with gaps similar to the arrangement of iron particles around a magnet on a laboratory table. The evolution of the rings takes tens of thousands of years, resulting in a disk with a thickness of ten meters.
- Quantum Locking: Quantum locking comes into play, causing the superconducting iced particles to be locked within a magnetic well at the magnetic equator plane. The locking mechanism involves the formation of Abrikosov vortex structures for superconductors. Even particles with a small fraction of superconductor material become locked within a three-dimensional magnetic well.

- Contributions to the Disk: The evolution of the rings may also receive contributions from other sources, such as collision-generated debris from the current moon, incoming meteorites, and geysers resulting from the magnetic coupling of Saturn and Enceladus.

- Relict of Early Magnetic Field: The rings are considered relics of the early days of the Saturn system's magnetic field, providing insights into the historical development of the planet's magnetic environment.

Conclusion:

This proposed mechanism suggests a unique interplay between Saturn's magnetic field, superconducting iced particles, and quantum locking, leading to the formation and stability of the iconic rings. The model not only provides a theoretical framework for the origin of Saturn's rings but also incorporates contributions from various celestial processes, adding complexity to the evolutionary history of the ring system. This interpretation presents Saturn's rings as a relict from the early magnetic field of the Saturn system, offering a novel perspective on their formation and persistence over astronomical timescales.

Totally frictionless magnetic bearing [5]

A totally frictionless magnetic bearing has been developed which supports a rotor in a contactless manner. The rotor is held in a magnetic potential well via repulsive forces only. Vertical and lateral restoring forces are provided to the rotor passively via permanent magnets in such an arrangement so as to support the weight of the rotor and provide it with a high degree of lateral stability. Axial stability of the rotor is provided by the use of an electromagnet which is controlled by a PID control loop. Information on the axial position of the rotor is provided to the circuit by use of an infrared LED and IR phototransistor. To prevent unwanted oscillations of the rotor's axial position from occurring, an oscillation sensor in the form of an inductive pick-up coil of high impedance provides signals to the oscillation sensing portion of the circuit, which in turn feeds the oscillation dampening circuit. The use of only repulsive forces in stabilizing the rotor means that there will be no eddy current losses or hysteresis losses. Such a frictionless magnetic bearing can, for example be used in rotational oscillation experiments and ultra-low loss watt-hour meters, which are of great importance to utility companies. When properly tuned, the total power requirements of the circuit is a mere 40mW, which is less than the 80 mW used by present day watt-hour meters.

Key Findings:

- Magnetic Potential Well: Repulsive magnetic forces create a potential well that holds the rotor in a contactless manner, eliminating friction.
- Permanent Magnets for Lateral Stability: Permanent magnets passively provide vertical and lateral restoring forces to support the weight of the rotor and enhance lateral stability.
- Electromagnet for Axial Stability: An electromagnet, controlled by a PID control loop, ensures axial stability of the rotor. This is crucial for precise control over the rotor's position.
- Position Sensing: Information on the axial position of the rotor is obtained using an infrared LED and IR phototransistor, enabling precise control over the rotor's position.
- Oscillation Sensing and Dampening: An inductive pick-up coil serves as an oscillation sensor, detecting any unwanted oscillations in the rotor's axial position. Signals from this sensor are fed to an oscillation dampening circuit to prevent oscillations.
- Energy Efficiency: The use of only repulsive magnetic forces minimizes losses due to eddy currents and hysteresis, ensuring high efficiency.

Conclusion:

This frictionless magnetic bearing technology presents a breakthrough in contactless rotor support, offering applications in experiments and utility meters with exceptional efficiency. The elimination of physical contact and the use of repulsive magnetic forces contribute to the reduction of energy losses, making it a valuable advancement in precision control systems.

First Room-Temperature Ambient-Pressure Superconductor [6]

This groundbreaking achievement marks the first successful synthesis of a room-temperature superconductor, denoted as LK-99. LK-99 exhibits superconductivity at ambient pressure, with a critical temperature (Tc) exceeding 400 K (127 °C).

Key Findings:

- Structural Characteristics: LK-99 possesses a modified lead-apatite structure, distinguishing it from previously known superconductors. The superconductivity of LK-99 is proven through various characteristics, including Critical temperature (Tc), Zero-resistivity, Critical current (I_c), Critical magnetic field (H_c), and the Meissner effect.
- Origins of Superconductivity: The superconductivity of LK-99 originates from minute structural distortion induced by a slight volume shrinkage of 0.48%. This unique property sets it apart from superconductors influenced by external factors such as temperature and pressure. The volume shrinkage is attributed to Cu2+ substitution of Pb2+(2) ions within the insulating network of Pb(2)-phosphate, generating stress in the structure.
- Structural Impact on Superconductivity: The stress induced by volume shrinkage transfers to Pb(1) of the cylindrical column, resulting in the distortion of the cylindrical column interface. This distortion creates superconducting quantum wells (SQWs) in the interface, contributing to the superconductivity of LK-99.
- Heat Capacity Model: Results from heat capacity measurements support a new model that explains the superconductivity of LK-99. This model considers the minute distorted structure and its impact on the interfaces.
- Unique Structural Feature: The ability of LK-99 to maintain and exhibit superconductivity at room temperatures and ambient pressure is attributed to its unique structure, allowing the preservation of minute distorted structures in the interfaces.

Significance:

The synthesis of LK-99 represents a significant milestone in the field of superconductivity. The achievement of room-temperature superconductivity at ambient pressure, coupled with the novel structural characteristics and the absence of external dependencies like temperature and pressure, opens new avenues for practical applications in various technological fields. The unique properties of LK-99 offer a promising foundation for further research and development in the realm of high-temperature superconductors.

CHAPTER 3: CONCEPT OF SUPERCONDUCTORS

3.1: Superconductivity

The history of superconductivity derives from a Dutch physicist named Heike Kamerlingh Onnes while exploring how different materials behave when cooled down to nearly absolute zero. Whilst in his experimentation, he observed a pattern of physical properties within certain materials that when cooled down to a certain temperature near absolute zero, the material loses all of its electrical resistance, thereby expelling the magnetic flux lines from entering the object. Any material sharing the same physical properties is referred to as a superconductor (Figure 3.1) In other words, a superconductor is a material that conducts electricity from one atom to another with zero electrical resistance. When the superconductor is in motion, the electricity will flow endlessly in a closed-loop.

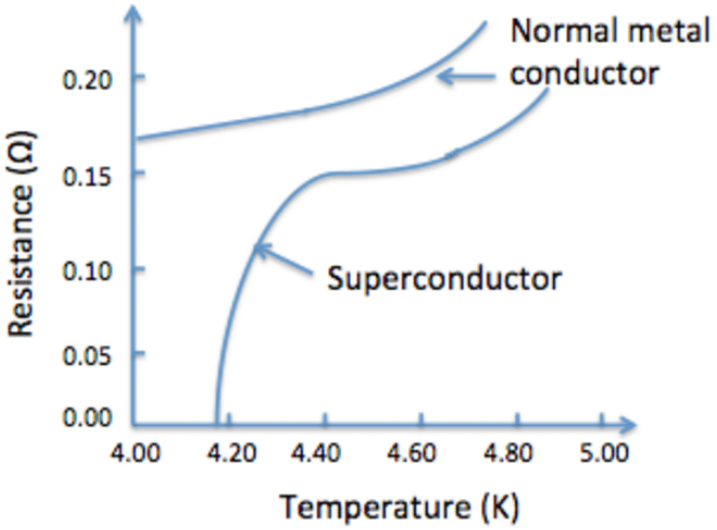

Fig 3.1: Resistance vs Temperature

There are a few distinctions between type-I and type-II superconductors. Their difference can be identified in the material's behavior under the application of an external magnetic field. Type-I superconductors mainly consist of metallic elements, including zinc, mercury, aluminum, and lead. Moreover, the transition to superconducting state happens instantly. Moreover, type-I superconductors oppose all flux from the material allowing no magnetic flux to penetrate the object. In other words, type-I superconductors fully demonstrate the Meissner effect. In type-II

superconductors, as the temperature decreases, the superconducting properties of the material increases as well. This can be seen in the image above (Figure 3.1) with a small curve slowly approaching zero electrical resistance once the temperature is below the critical temperature $\mathbf{T_c}$. Furthermore, type-II superconductors do not fully exhibit the Meissner effect. A type-II superconductor will only expel the magnetic field when the first maximum magnetic field strength, $\mathbf{H_c}$, is reached. Once the first $\mathbf{H_c}$ is reached, vortices appear, diminishing all superconducting properties in that region. Around the vortices, the current starts to circulate. Although vortices formed, the rest of the superconductor is still in a superconducting state. The presence of the vortices allows magnetic flux to penetrate through the material enabling a quantum phenomenon known as flux pinning, otherwise known as quantum locking. Hence, type-II superconductors are primarily used for superconducting magnets and further experimentation for potential uses in the future.

Table 3.1: Difference b/w Type-I and Type-II Superconductors

Type-I Superconductors	**Type-II Superconductors**
Metallic elements.	Alloys, composites, metal oxide ceramics, or perovskites.
Lower critical temperatures.	Higher critical temperatures.
Sharp transition to critical temperature.	A gradual transition to critical temperature.
Type-I superconductors work via cooper-pairs (BCS Theory).	The BCS theory cannot be applied to explain the behavior of type-II superconductors.

3.2: Zero Resistance at low temperatures

It had been known for many years that the resistance of metals fell gradually when cooled below room temperature, but it was not known what limiting value the resistance would approach if the temperature were reduced to very close to absolute zero. The era of low-temperature physics began in 1908 when Dutch physicist Heike Kamerlingh Onnes first liquefied helium, which boils at 4.2 K. Three years later, Onnes passed a current through a very pure mercury wire and measured its resistance as he steadily lowered the temperature. Much to his surprise, there was no leveling off of the resistance until the temperature reached 4.2 K, at which point the resistance suddenly vanished. Current was flowing through the mercury wire and nothing was stopping it the resistance was zero. Onnes called this new state of zero resistance superconductivity. In 1913, Onnes was awarded the Nobel Prize in physics for the study of matter at low temperatures and the liquefaction of helium. Soon afterwards, many other metals were found to exhibit zero resistance when their temperatures were lowered below a certain characteristic temperature, called the critical temperature, or T_c.

The importance of this discovery to the scientific community as well as its commercial potential was clear. An electrical conductor with no resistance could carry current to any distance with no losses.

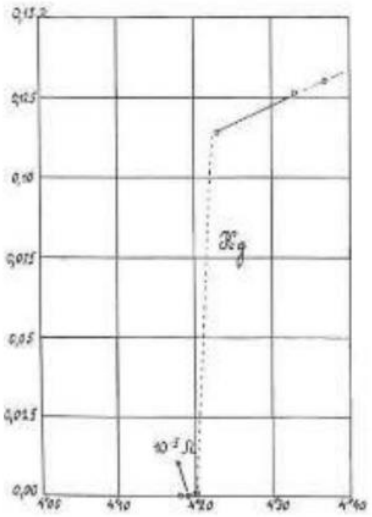

Fig 3.2: The original graph from Onnes's publication from 1911

3.3: The Meissner effect

The magnetic properties of superconductors are as dramatic as their complete lack of resistance. In 1933, Hans Meissner and Robert Ochsenfeld studied the magnetic behavior of superconductors and found that when certain ones are cooled below their critical temperatures, they have an interesting property of expelling a magnetic field. They discovered that a superconductor will not allow a magnetic field to penetrate its interior. It achieves this by producing a "magnetic mirror," surface currents which produce a magnetic field that exactly counters the external field. The phenomenon of the expulsion of magnetic fields from the interior of a superconductor is known as the Meissner effect.

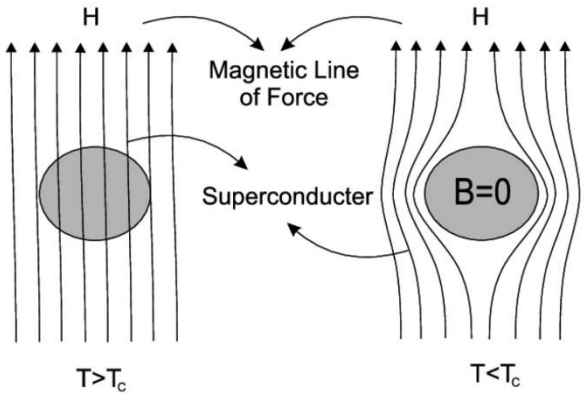

Fig 3.3: Meissner effect

3.4: Physics behind superconductivity

According to classical physics, part of the resistance of a metal is due to collisions between free electrons and the crystal lattice's vibrations (called phonons). In addition, part of the resistance is due to scattering of electrons from defects or impurities in the metal. Soon after the discovery of superconductivity, scientists recognized that this classical model could never explain the superconducting state because the electrons in a material always suffer some collisions, and therefore resistivity can never be zero. In 1957, three American physicists at the University of Illinois, John Bardeen, Leon Cooper, and Robert Schrieffer, developed a model that has since stood as a good mental picture of why superconductors behave as they do. The central feature of the theory is that two electrons in the superconductor are able

to form a bound pair called a Cooper pair if they somehow experience an attractive interaction between them. This notion, at first sight, seems counterintuitive since electrons normally repel one another because of their similar charges. However, a net (or effective) attraction can be achieved if the electrons interact with each other via the motion of the crystal lattice as the lattice structure is momentarily deformed by a passing electron. The second electron (the Cooper pair partner) comes along and is attracted by the displaced ions.

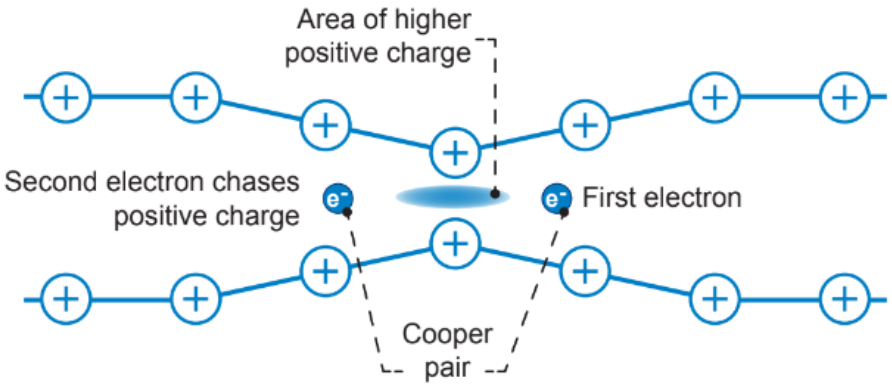

Fig 3.4: Electrons inside the atom lattice

Figure 3.4 shows two electrons inside the atom lattice. The existence of electron 1 causes nearby ions to move inward toward the electron, resulting in a slight increase in the concentration of positive charge in this region. Electron 2 (the second electron of the Cooper pair) is attracted to the distorted (positively charged) region. The net effect is a weak delayed attractive force between the two electrons, resulting from the motion of the positive ions. Area of higher positive charge Second electron chases positive charge e^- e^- First electron Cooper pair The interaction between a Cooper pair is transient. Each electron in the pair goes on to form a Cooper pair with other electrons, and this process continues with the newly formed Cooper pair so that each electron goes on to form a Cooper pair with other electrons. The end result is that each electron in the solid is attracted to every other electron forming a large network of interactions. For the advanced reader: The new pair acts as a new effective particle that has completely different properties than the original electrons. Unlike their creators, the new particles are Bosons (named after the Indian physicist, Satyendra Nath Bose) which possess the ability to occupy the same energy state. The Pauli

Exclusion Principle does not apply to Bosons and so all the Cooper pairs condensate to occupy the same lowest energy level available. This new state has substantially lower energy and hence highly stable. Cooper pairs passing current inside the Superconductor will not shift their energy upon collision and hence no energy dissipation will occur. The model is expressed in terms of advanced ideas of the science of quantum mechanics, but the main idea of the model suggests that electrons in a superconductor condense into a quantum ground state and travel together collectively and coherently. In 1972, Bardeen, Cooper and Schrieffer received the Nobel Prize in Physics for their theory of superconductivity, which is now known as the BCS theory, after the initials of their last names.

CHAPTER 4: MATERIAL SELECTION

4.1: Superconductor Material

The use of superconductors is essential to the potential development of future transportation systems, also the key to carrying out this experiment. Superconductivity is a phenomenon that allows materials, known as superconductors, to conduct electricity from one atom to another with zero electrical resistance. As previously mentioned, there are two types of superconductors. The difference between both categories can be identified by their magnetic behavior and their transition to the superconducting state. In the chart below, there is a list of type I and type II superconductors of different materials, with their critical temperature.

Table 4.1: Critical Temperatures of different Materials

TYPE - I		**TYPE - II**	
NAME	**CRITICAL TEMP**	**NAME**	**CRITICAL TEMP**
Lead (Pb)	7.196 K	$Sn_6Sb_6Ba_2MnCu_{13}O_{26+}$	110 C^o
Lanthanum (La)	4.88 K	$Sn_5Sb_5Ba_2MnCu_{11}O_{22+}$	95 C^o
Tantalum (Ta)	4.47 K	$YBa_3Cu_4O_x$	177 K
Mercury (Hg)	4.15 K	$YBa_2Cu_3O_7$	92 K
Tin (Sn)	3.72 K	$TmBa_2Cu_3O_7$	90 K

The most suitable superconductor for this exploration was the YBCO crystal. YBCO is an abbreviation for Yttrium Barium Copper Oxide.

A Brief Knowledge about YBCO:

The YBCO superconductor is often used for superconducting magnets and further experimentation. It is a type II superconducting copper oxide. This compound is well known in the field of superconductivity because it was one of the first superconductors to have a T_c higher than liquid nitrogen (77 K). Prior superconductors, demonstrated superconducting properties at a critical temperature at 4 K, the boiling point of liquid helium. 16 Under optimal

conditions of stoichiometry without applied field, solid YBCO has a critical temperature of 92 K. This high critical temperature, characteristic of type II superconductors, made it possible to dispense of liquid helium cryogenics, which imposed temperatures below 4 K, and to use cryogenics with liquid nitrogen, thereby considerably reducing the cost of operation of materials to transition a conductor to a superconducting state.

YBCO Structure (Chemically):

YBCO has a critical temperature of 92 K, the first known superconductor to transition into a superconducting state at 77 K. The $YBa_2Cu_3O_{7-x}$ has two layers of CuO_2. These chains are the key reason for the superconductivity in the material. YBCO is synthesized by heating a mixture of metal carbonates at temperatures around 1000 K and 1300 K.

$$4BaCO_3 + Y_2(CO_3)_3 + 6CuCO_3 + (\tfrac{1}{2} - x)O_2 \rightarrow 2YBa_2Cu_3O_{7-x} + 13CO_2$$

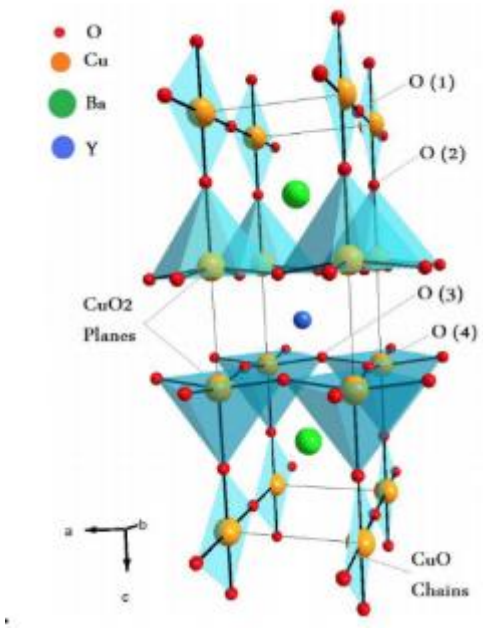

Fig 4.1: YBCO Structure

4.2: Permanent Magnet Material

There are four classes of modern commercialized magnets, each based on their material composition. Within each class is a family of grades with their own magnetic properties. These general classes are:

- Neodymium Iron Boron (NdFeB)
- Samarium Cobalt (SmCo)
- Ceramic
- Alnico

NdFeB and SmCo are collectively known as rare-earth magnets because they are both composed of materials from the Rare Earth group of elements.

- Neodymium Iron Boron (general composition $Nd_2Fe_{14}B$, often abbreviated to NdFeB) is the most recent commercial addition to the family of modern magnet materials. At room temperatures, NdFeB magnets exhibit the highest properties of all magnet materials.
- Samarium Cobalt is manufactured in two compositions: Sm_1Co_5 and Sm_2Co_{17} - often referred to as the SmCo 1:5 or SmCo 2:17 types. 2:17 types, with higher H_{ci} values, offer greater inherent stability than the 1:5 types.
- Ferrite, also known as ceramic magnets (general composition $BaFe_2O_3$ or $SrFe_2O_3$) have been commercialized since the 1950s and continue to be extensively used today due to their low cost. A special form of Ferrite magnet is "Flexible" material, made by bonding Ferrite powder in a flexible binder.
- Alnico magnets (general composition Al-Ni-Co) were commercialized in the 1930s and are still extensively used today.

These materials span a range of properties that accommodate a wide variety of application requirements. The following is intended to give a broad but practical overview of factors that must be considered in selecting the proper material, grade, shape, and size of magnet for a specific application. The chart below shows typical

values of the key characteristics for selected grades of various materials for comparison. These values will be discussed in detail in the following sections.

Table 4.2: Property - Symbol - Unit

Property	**Symbol**	**Unit**
Flux Density	B_r	gauss
Coercive Force	H_c	oersteds
Intrinsic Coercive Force	H_{ci}	oersteds
Energy Density	$(BH)_{max}$	kJ/m^3

Table 4.3: Magnetic Properties

Material	**B_r**	**H_c**	**H_{ci}**	**$(BH)_{max}$**
NdFeB	12,800	12,300	21,000	40
SmCo	10,500	9,200	10,000	26
Ceramic	2300	150	260	8.35
Alnico	12,500	640	640	5.5

The two most important properties form a permanent magnet for quantum locking applications are flux density and energy density. From the above table (4.3) the highest Flux density and energy density is of NdFeB.

The most suitable permanent magnet from this exploration was NdFeB also known as Neodymium magnet.

Neodymium magnets are known to be the strongest magnets in the world. Its magnetic flux density depends on the dimensions of the magnet. It is a permanent magnet, an object that produce a magnetic field from within the material. Inside the material, there are electrons and the nucleus of the atom, which both act like small magnets. They have magnetic fields innate the molecules themselves. Another fashion the magnets generate a magnetic field is through the orbital motion of the electrons as they move about the core, the nucleus. Hence, the magnetic fields are

determined through the aggregations of the nuclear gyrations, the electron turns, and the periods of the electrons themselves.

Determining the Flux density of the magnet:

The magnetic flux density is mainly known as the "B field", also "magnetic induction". The magnetic flux density is measured in tesla or gauss, where 10 000 gauss is equal to 1 tesla. However, due to the principles of SI units, the official units for measuring the flux density is in tesla. There are no simple calculations that could be used to quantify the flux density of permanent magnets due to their various shapes and forms, including block, cylinder, ring, and sphere magnets. For the purpose of this exploration, neodymium block magnets were used. Thus, the equation needed to calculate the flux density is of the following:

- Cylindrical Magnets:

$$B_x = \frac{B_r}{2}\left(\frac{(L+X)}{\sqrt{R^2+(L+X)^2}} - \frac{X}{\sqrt{R^2+X^2}}\right)$$

- Rectangular Magnets:

$$B = \frac{B_r}{\pi}\cdot\left(\arctan\left(\frac{L\cdot W}{2z\sqrt{4z^2+L^2+W^2}}\right) - \arctan\left(\frac{L\cdot W}{2(D+z)\sqrt{4(D+z)^2+L^2+W^2}}\right)\right)$$

- For Ring Shaped Magnets:

$$\frac{B_r}{2}\left(\left(\left(\frac{L+x}{\sqrt{R^2+(L+x)^2}}\right)-\left(\frac{L+x}{\sqrt{r^2+(L+x)^2}}\right)\right)-\left(\left(\frac{x}{\sqrt{R^2+x^2}}\right)-\left(\frac{x}{\sqrt{r^2+x^2}}\right)\right)\right)$$

For the project we are only focusing on rectangular magnets as it is best suited for quantum locking.

B_r = Residual Flux Density

z = Distance from the pole face to the superconductor

L = Length of the block permanent magnet

W = Width of the block permanent magnet

D = Height of the magnet

In this equation there are two constants B_r and π. The next variables are L, W, D, and z. These variables are representing the dimensions of the permanent magnet as seen in Figure 4.2.

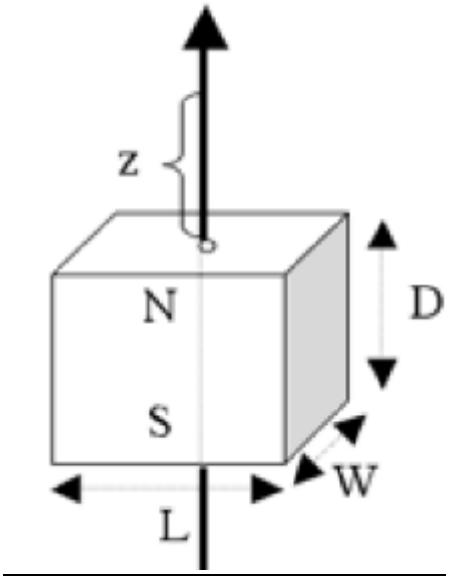

Fig 4.2: Magnet representation

Table 4.4: Flux Density calculation (INPUT)

INPUT					
L	W	D	Br	z	Br/π
0.01	0.01	0.01	1.29	0.015	0.410828
m	m	m	T	m	

Table 4.5: Flux Density calculation (OUTPUT)

OUTPUT			
arctan1	arctan2	Bx	Bx
0.100167	0.038471	0.025347	253.4661
		Tesla	Gauss

CHAPTER 5: GOVERNING EQUATIONS

5.1: INTRODUCTION

The force of interaction between a levitating superconductor and the system generating the magnetic field consists of the levitation force and the guidance or lateral force that secures the stability of levitation. The lateral and levitation forces depend on the distance, Zcp, between the field source and the superconductor when the superconductor is cooled down in opposite ways: the larger the value of Zcp, the larger is the levitation force and the lower is the restoring force [13]. In some cases, there is a threshold for Zcp above which levitation is unstable [14]. To date, different numerical and analytical approaches have been proposed for determining these forces. As in the case of any electromagnetic setup, numerical simulations generally employ finite elements methods (FEMs) for solving Maxwell's differential equations. Superconductivity is accounted for by introducing a so-called power law between the electric field, E, and the current density, J. This law generally takes the form

$$E = E_C \left(\frac{J}{J_c}\right)^n \tag{1}$$

where Ec is usually the electric field criterion employed for defining the superconductor critical current density, Jc, whereas the exponent n is proportional to the activation energy of vortex depinning. FEMs allows determining $\vec{J}$ as well as the field, $\vec{B}$, generated by the magnetic source everywhere in the superconductor. The force of interaction with the magnetic system is written as

$$\vec{F} = \int_V \vec{J} \times \vec{B}\, dv \tag{2}$$

where v is the superconductor volume.

5.2 CALCULATION OF THE LEVITATION FORCE

Due to the symmetry of the system $\vec{m}$ is parallel to the disc axis, Oz, and we consider only the vertical component, mz. Based on Eq. (3), we write the levitation force, Fz, as

$$F_z(z) = m_z \frac{\partial B_z}{dz} \tag{3}$$

where Bz is the vertical component of the magnet field along the axis of the sample. However, the field gradient generated by the magnet is nonuniform on the scale of the thickness of the bulk. Consequently, $\partial Bz \partial Z$ is replaced in Eq. (4) by its value averaged on the thickness, t, of the part of the superconductor carrying the shielding currents:

$$\frac{\partial B_z}{\partial z} = \frac{1}{t} \int \frac{\partial B_z}{\partial z} dz \tag{4}$$

The magnetic moment, mz, can be written according to the expression proposed by Brandt for the magnetic moment of a disk in an axial field [32]. Since the shielding currents are due to the modulation of the external field, here we consider that the field to be taken into account is the difference between the fields at the locations Z and Zcp. These fields are nonuniform in the bulk, and in the framework of our mean-field approximations, we take their mean value calculated over the thickness t. As the magnet goes down, the resulting magnetic moment is

$$m_z = -\frac{2}{3} J_c t R^3 \left[cos^{-1} \left(\frac{1}{cosh\left(\frac{2\Delta B_a}{\mu_0 J_c t}\right)} \right) + \frac{sinh\left|\frac{2\Delta B_a}{\mu_0 J_c t}\right|}{cosh^2\left(\frac{2\Delta B_a}{\mu_0 J_c t}\right)} \right] \tag{5}$$

Where

$$\Delta B_a = \langle B_z(Z) \rangle - \langle B_z(z_{cp}) \rangle \tag{6}$$

where $\langle Bz(Z_{cp}) \rangle$ and $\langle Bz(Z) \rangle$ are the values of the vertical components of the fields applied along the superconductor axis at the cooling point and at the distance *Z*, averaged over the thickness *t*. Finally, the levitation force during the downward motion of the magnet takes the form

$$F_z(z) = m_z \frac{\partial B_z}{dz} \tag{7}$$

When the magnet motion is reversed at Zmin, the shielding currents present in the superconductor do not disappear. As a result, during the upward motion, the magnetic moment comprises two components

$$m_{max} = -\frac{2}{3}J_c t R^3 \left[cos^{-1}\left(\frac{1}{cosh\left(\frac{2\Delta B_{max}}{\mu_0 J_c t}\right)} \right) + \frac{sinh\left|\frac{2\Delta B_{max}}{\mu_0 J_c t}\right|}{cosh^2\left(\frac{2\Delta B_{max}}{\mu_0 J_c t}\right)} \right] \quad (8)$$

And

$$m_b = \frac{2}{3}J_c t R^3 \left[cos^{-1}\left(\frac{1}{cosh\left(\frac{2\Delta B_b}{\mu_0 J_c t}\right)} \right) + \frac{sinh\left|\frac{2\Delta B_b}{\mu_0 J_c t}\right|}{cosh^2\left(\frac{2\Delta B_b}{\mu_0 J_c t}\right)} \right] \quad (9)$$

Where

$$\Delta B_{\max} = \langle B_z(z_{\min})\rangle - \langle B_z(B_{cp})\rangle \quad (10)$$

And

$$\Delta B_b = \langle B_z(Z)\rangle - \langle B_z(Z_{\min})\rangle \quad (11)$$

The moment, $\vec{m}max$, is generated by the currents that flow in the superconductor when the motion of the magnet is reversed. Currents resulting in the moment, $\vec{m}b$, flow in the sample to compensate for the field variations between Zmin and Z. The currents creating the moments $\vec{m}max$ and $\vec{m}b$ flow in opposite directions, suggesting that they are located in different parts of the superconductors. While it is reasonable to suppose that the shielding currents flow in the part of the superconductor of thickness, t, that is facing the magnet during its downward motion, we have assumed that they flow in the areas during the upward motion. As a consequence, Fz takes the form

$$F_z = m_{\max}\left\langle \frac{\partial B_z(z+t)}{\partial z} \right\rangle + m_b\left(\frac{\partial B_z(Z)}{\partial Z}\right) \quad (12)$$

for this part of the cycle. Otherwise, the measurements and calculations reported in [25, 33] result in $t \leq h2$ for all the investigated samples and we have no insights on the current distribution for $t > h2$. As a consequence, the model is valid for force cycles that can be reproduced with $t \leq h2$ only. Since previous measurements have shown

that t increases with increasing temperature [33], this constraint sets a high temperature limit for the model.

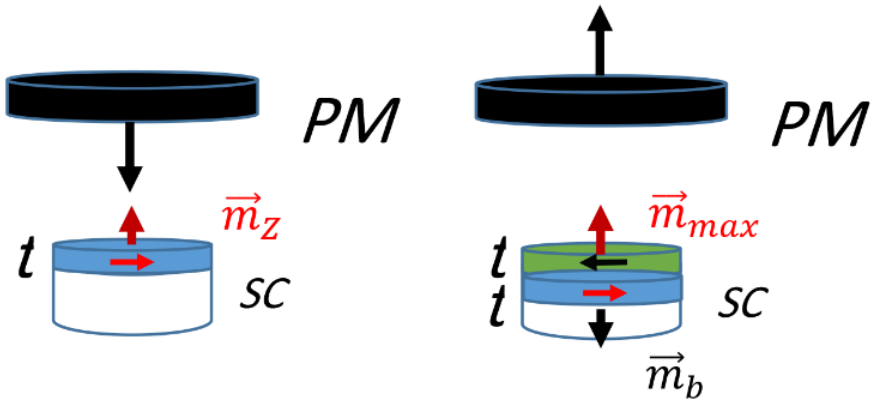

Fig 5.1: Assumed locations of the currents in the superconductor

For the calculations, since the surface current density of the sample JSC=Jct is present in Eqs. (5), (8), and (9), we take this quantity and the thickness, t, as the fitting parameters to reproduce the measurements with Eqs. (7) and (12). Consequently, the fitting process gives JSC, t, and Jc. Figure 5.1 shows the levitation forces between an MgB2 cylinder, with a diameter D = 59.6 mm and thickness h = 9.8 mm, and a 70 mm diameter and 30 mm thick NdFeB magnet measured at various temperatures. The superconductor was cooled down at a distance of Zcp = 37 mm from the magnet.

5.3: LATERAL FORCE AND STABILITY

We consider only the superconducting cylinders with $D \gg h$. Consequently, a possible radial component of $\vec{m}$ is much smaller than the vertical one, and we do not take it into account. Otherwise, we take the sign of $\partial Fr \partial r$ near r = 0 as an indicator of stability. This quantity is positive for two magnets with opposite magnetization and negative if the levitation is stable. Using Eq. (3), we have

$$F_r = m_z \frac{\partial B_r}{\partial z} \tag{13}$$

Since the magnetic field is generated by an external source, we have

$$\vec{\nabla} \times \vec{B} = 0 \text{ and } \frac{\partial B_r}{\partial z} = \frac{\partial B_z}{\partial r} \tag{14}$$

and *Fr* can be written as

$$F_r = m_z \frac{\partial B_z}{\partial r} \tag{15}$$

The magnetic moment, *mz*, takes the same form as in Eq. (6). However, since the system is not axisymmetric for r ≠ 0, we assume that

$$\Delta B_a = \langle B(0, Z_{cp}) \rangle - B_\phi(r, Z) \tag{16}$$

where

$$B_\phi(r, Z) = \frac{\phi(r, z)}{\pi \frac{D_{sc}^2}{4}} \tag{17}$$

where $\phi(r,Z)$ is the flux of the mean value on the thickness, *t*, of the field threading the disc when the magnet is at the location (r,Z). There are various techniques permitting one to calculate this quantity. As an example, in Appendix I, we describe the technique we have used for reproducing the measurements reported in Figure 6 and Figure 8. Otherwise, the modulation of *r* results in that of $B\phi(r,Z)$ only. Consequently, *Fr* can be written as

$$F_r = m_z \frac{\partial B_\phi(r, Z)}{\partial r} \tag{18}$$

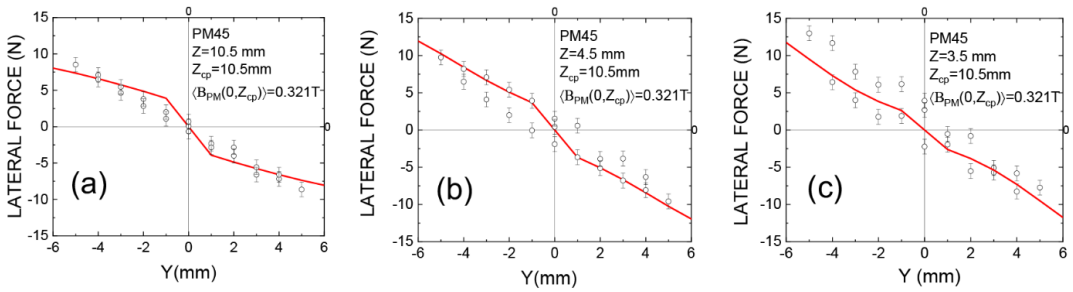

Fig 5.2: Lateral force (Fy) at different gaps

CHAPTER 6: FORCE CALCULATION

6.1: QUICKFIELD

QuickField™ is a very efficient Finite Element Analysis package for electromagnetic, thermal, and stress design simulation with coupled multi-field analysis. It combines a family of analysis modules using the latest solver technology with a very user-friendly model editor (pre-processor) and a powerful postprocessor.

QuickField requires no training - you may start using it as soon as it is installed on your computer, without knowing the mathematical algorithms used and details of their implementation.

It is a native Windows® application, which was designed for this platform only. It fully utilizes the advantages of a modern operational environment. It is very compact, yet powerful, and can be used for many design applications. QuickField can be effectively applied to many engineering tasks. Most often, it is used in the design of electric motors, turbine generators, actuators, speakers, transformers, induction heating systems, transmission lines and other complex electrical and electromechanical devices. We have prepared tables of QuickField options that describe how it can be used in specific design problems.

APPLICATIONS:

The application of QuickField is not restricted to this list.

Superconductors	High voltage systems	PCB design
Building insulation	EMC analysis	Sensors
Cables	Induction heating systems	Speakers
Capacitors	Insulators	Thermal models
Electrical machines	Magnetic systems	Transformers
Electron-ion optics	Mechanical devices	Actuators

6.2: MODEL

In order to analyse the forces between the superconductor and magnet, our approach begins with the utilization of SolidWorks to construct detailed models of both components. SolidWorks provides a robust platform for precise and comprehensive 3D modelling, ensuring accurate representations of the superconductor and magnet geometries. Subsequently, these models are seamlessly imported into Quick Field software, which facilitates electromagnetic simulations and analysis.

Dimensions:

Superconductor:

Width: 10mm

Diameter: 42mm

Magnet:

Width: 10mm

Diameter: 42mm

Air:

Diameter: 150mm

Initial Distance between superconductor and magnet: 10mm

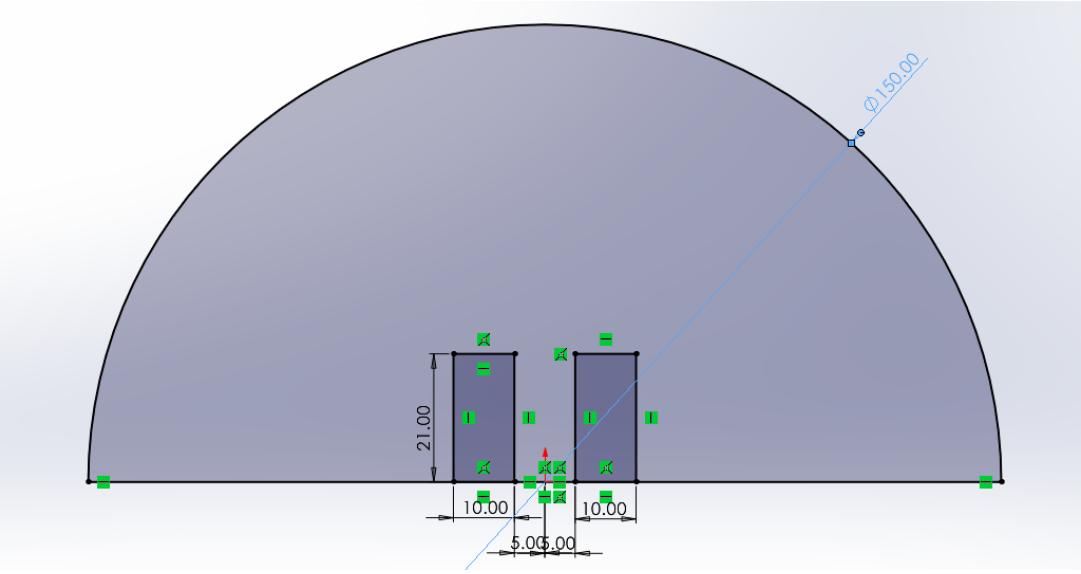

Fig 6.1: Sketching of superconductor, magnet and air model

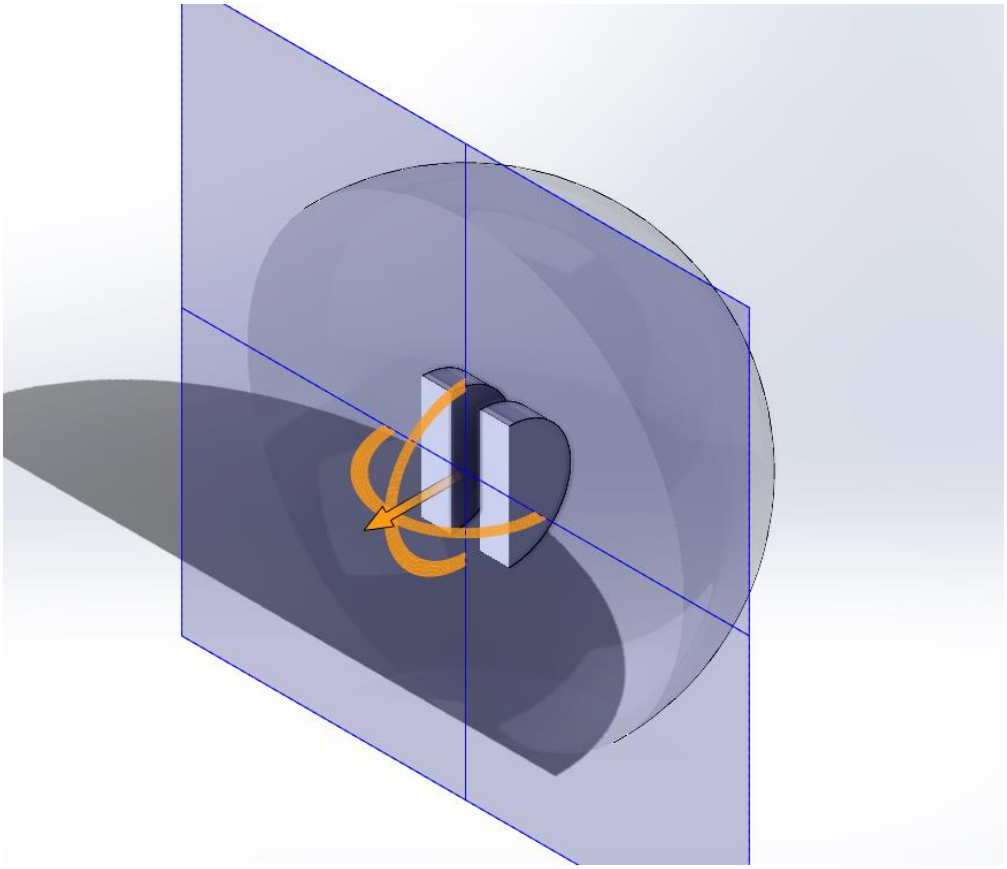

Fig 6.2: Section view of the apparatus

6.3: SIMULATION

STEP 1:

First, to initiate our analysis, we open the Quick Field software, a powerful tool for electromagnetic simulations. Upon launching the software, we proceed by selecting "New Problem" from the menu. Here, we are prompted to provide a filename for our project. In line with our focus on the superconductor and magnet interaction, we assign the filename as "superconductor" to reflect the essence of our investigation. With the filename set, we advance to the next step, ready to embark on our exploration of the electromagnetic phenomena at play within this system. This initial setup stage within Quick Field marks the commencement of our analytical journey, guiding us towards a deeper understanding of the forces and dynamics governing superconductor-magnet interactions.

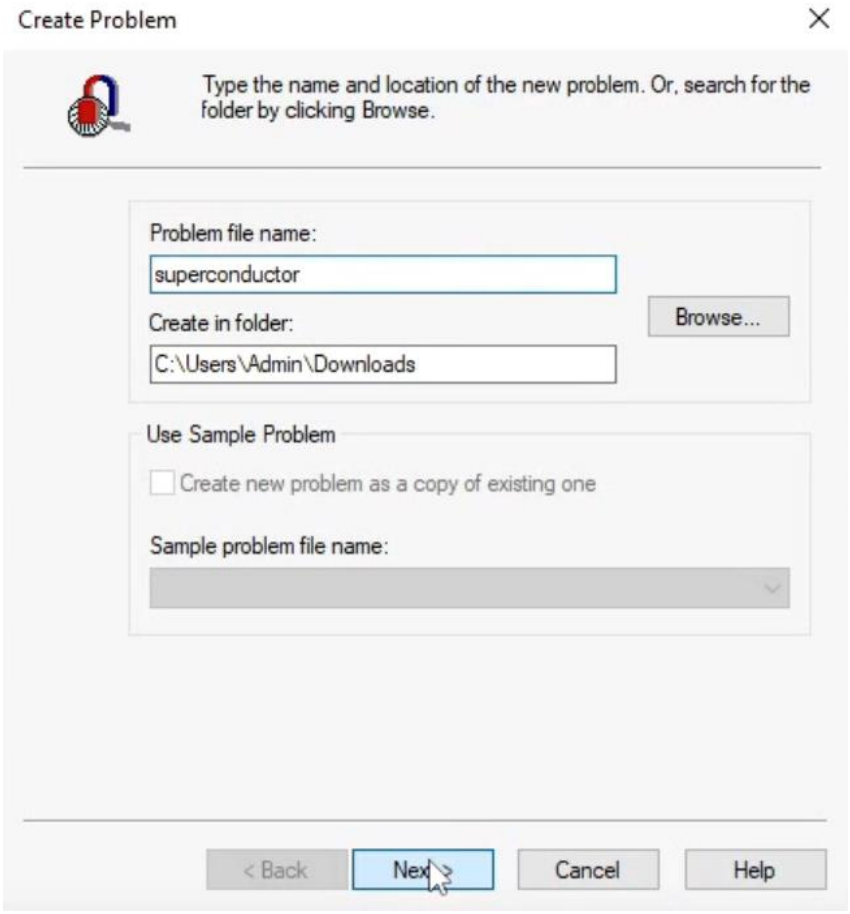

Fig 6.3: Step 1 (File name)

STEP 2:

In the second step of our analysis process, we navigate within the Quick Field software to select the appropriate problem type. Given our investigation involves the interaction between a magnet and a superconductor, we opt for the "Magnetostatics" problem type to accurately capture the static magnetic field behavior. Within the model class options, we choose "Axisymmetric" to leverage the symmetry inherent in our setup, streamlining computations while maintaining accuracy. For consistency and ease of interpretation, we designate millimeters as our preferred length units. Additionally, we select the Cartesian coordinate system to facilitate straightforward visualization and analysis. To ensure a balance between computational efficiency and accuracy, we opt for the "Normal" precision setting. With these parameters configured, we proceed by selecting "Next," advancing further into our analytical journey within Quick Field.

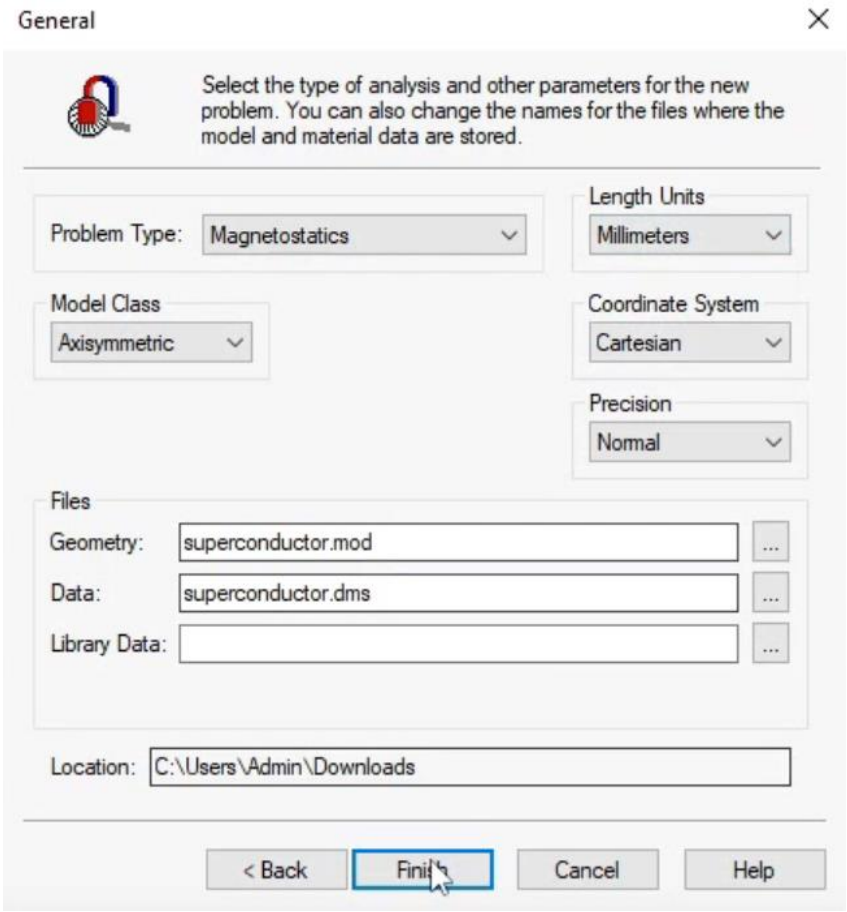

Fig 6.4: Step 2 (type of analysis)

STEP 3:

In the third step of our analytical process, we seamlessly integrate our SolidWorks model into the Quick Field software environment. Leveraging the convenient shortcut of "Ctrl+Alt+W," we initiate the importation process. This feature streamlines our workflow, allowing for efficient transfer of the meticulously crafted SolidWorks model into Quick Field. By importing the model directly, we ensure continuity and accuracy in our analysis, as the detailed geometrical representations generated in SolidWorks serve as the foundation for our electromagnetic simulations. This seamless integration not only enhances our productivity but also facilitates a cohesive approach to our investigation, enabling us to explore the complex interactions between the superconductor and magnet with precision and reliability.

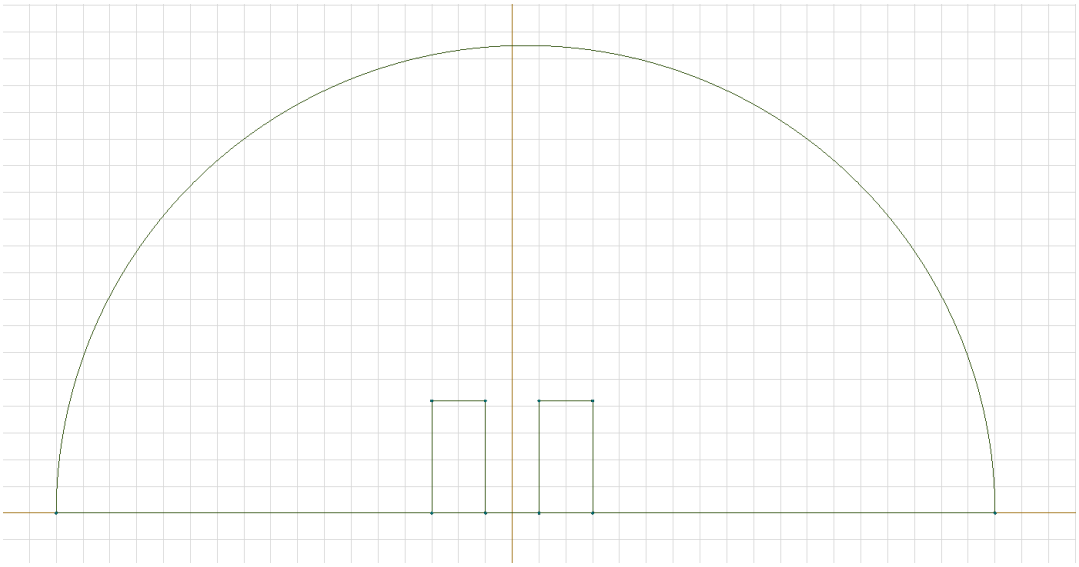

Fig 6.5: Step 3 (import Solidworks model into Quickfield)

STEP 4:

In step 4, we define the properties of the air section in our model using Block Label. We set the relative permeability to 1 and coercive force magnitude to zero, reflecting air's non-magnetic nature. Upon confirmation, we proceed with our analysis.

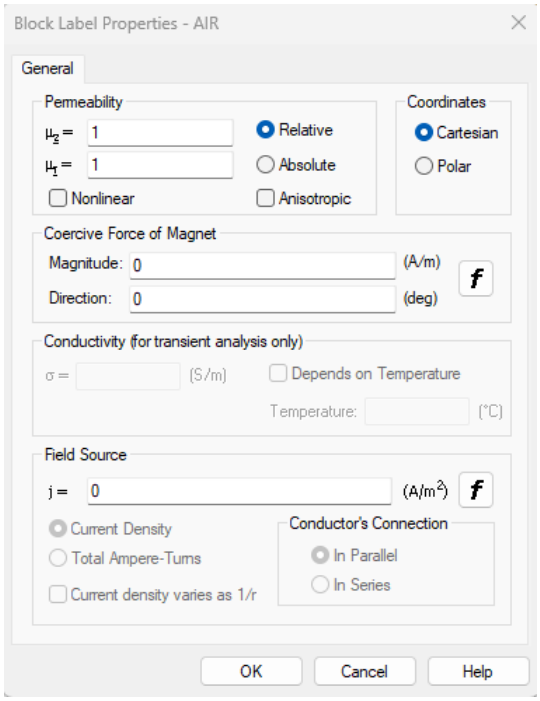

Fig 6.6: Step 4 (properties of air)

STEP 5:

In step 5 of our analysis, we focus on delineating the properties of the permanent magnet, specifically a neodymium magnet in our case. Using the Block Label functionality in Quick Field, we set the parameters to accurately represent the magnet's characteristics. Initially, we assign a relative permeability of 1, as neodymium magnets exhibit high magnetic permeability. Subsequently, we specify the magnitude of coercive force for the magnet, setting it at 978,802.9 A/m, which translates to approximately 12,300 oersteds. This value reflects the magnet's resistance to demagnetization. Once these properties are defined, we confirm our selections by clicking "OK," ensuring that our simulations accurately reflect the behavior of the neodymium magnet within the electromagnetic environment under study.

NOTE : 1 oersted = 79.5 A/m

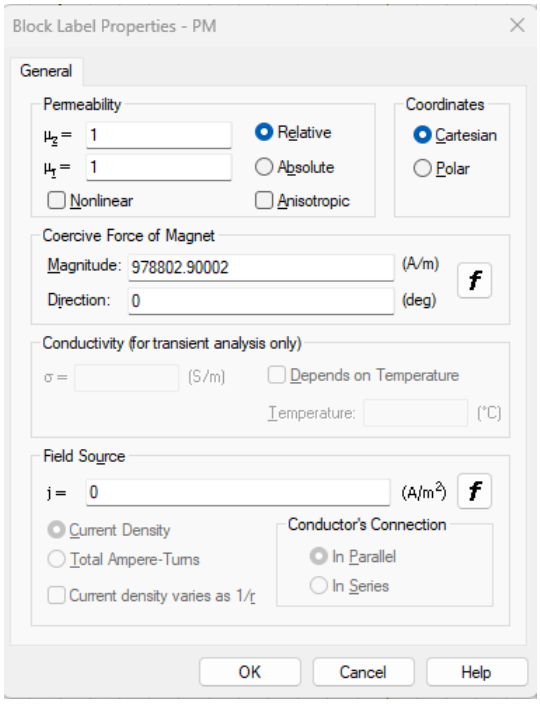

Fig 6.7: Step 5 (properties of permanent magnet)

STEP 6:

In step 6, we define the properties of the superconductor. Despite software limitations preventing a permeability value of zero, we assign a very small value of 1e-5. This

reflects the near-zero permeability characteristic of superconductors. This adjustment allows for an accurate representation of the superconductor's behavior in our simulations.

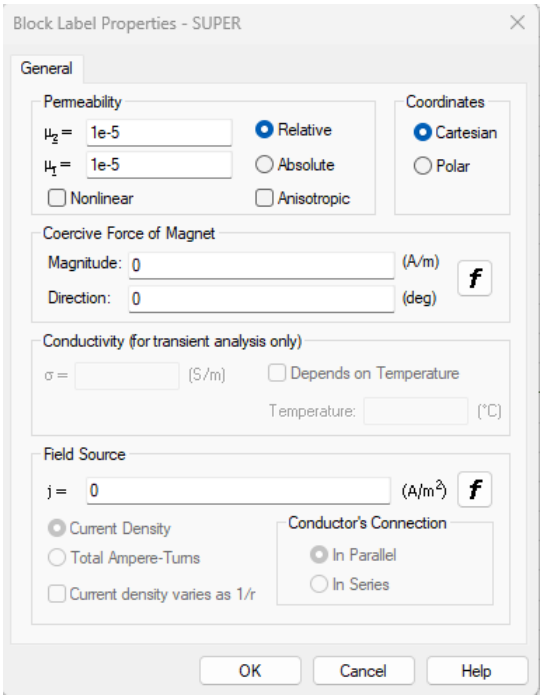

Fig 6.8: Step 6 (properties of superconductor)

STEP 7:

In step 7 of our analysis, we undertake the task of mesh generation to refine the representation of our geometry within Quick Field. This crucial step involves selecting the entire model and generating a fine mesh comprising nearly 4000 elements. By employing a fine mesh, we ensure that our simulation captures intricate details and nuances within the geometry, enhancing the accuracy and reliability of our results. This meticulous approach to mesh generation enables us to effectively capture the complex electromagnetic interactions between the superconductor, magnet, and surrounding components. With the mesh in place, we are poised to conduct our simulations with confidence, confident in the fidelity of our model and the insights it will provide into the behavior of the system under study.

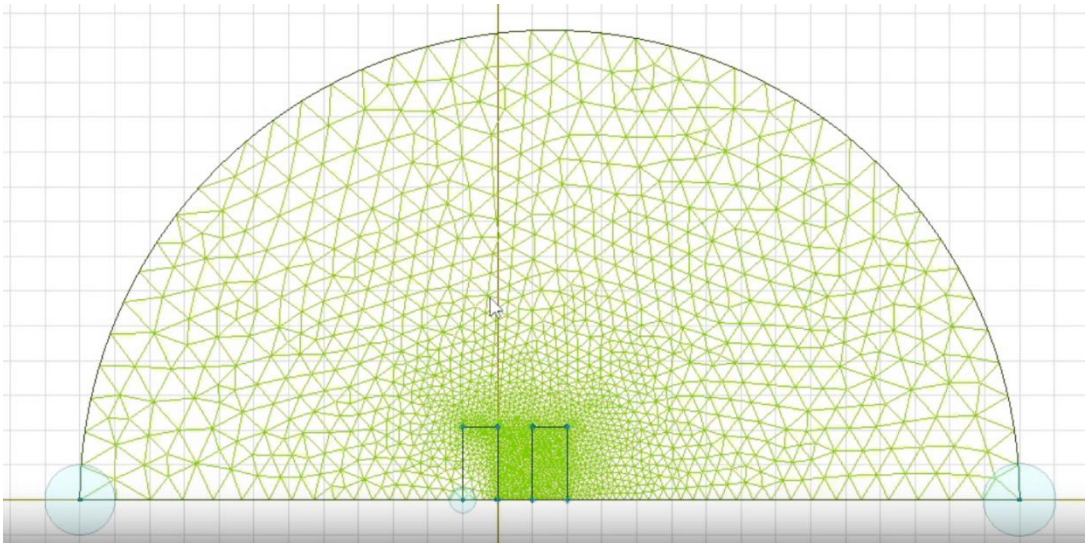

Fig 6.9: Step 7 (mesh)

STEP 8:

In step 8, we save the configured problem and then initiate the simulation by clicking on the "solve" button. This action prompts Quick Field to iterate through all finite elements, generating results and analyzing electromagnetic interactions.

6.4: RESULT

We have conducted an analysis to examine the variation in the force exerted on the superconductor as the distance between the magnet and superconductor is altered. The results of this investigation are presented in the table below, showcasing findings from five distinct cases. Through systematic experimentation and simulation within Quick Field, we have been able to quantify the influence of varying distances on the forces involved in the interaction between the superconductor and magnet. These findings provide valuable insights into the dynamics of this relationship, shedding light on how changes in distance impact the behavior and performance of superconductors within magnetic environments. Such insights are crucial for informing the design and optimization of systems utilizing superconducting materials, contributing to advancements in various technological domains.

Table 6.1: Result for 5 different cases

	Gap (mm)	Force on superconductor (N)
CASE 1	2	34.584
CASE 2	4	24.307
CASE 3	6	16.674
CASE 4	10	7.8707
CASE 5	14	3.9091

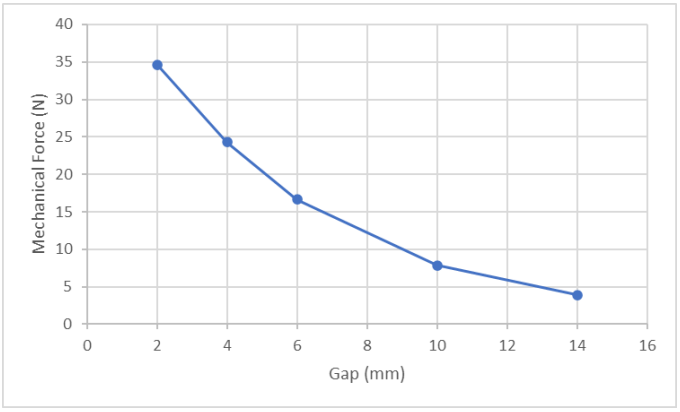

Fig 6.10: Variation in Force on Superconductor with Distance

CASE 1:

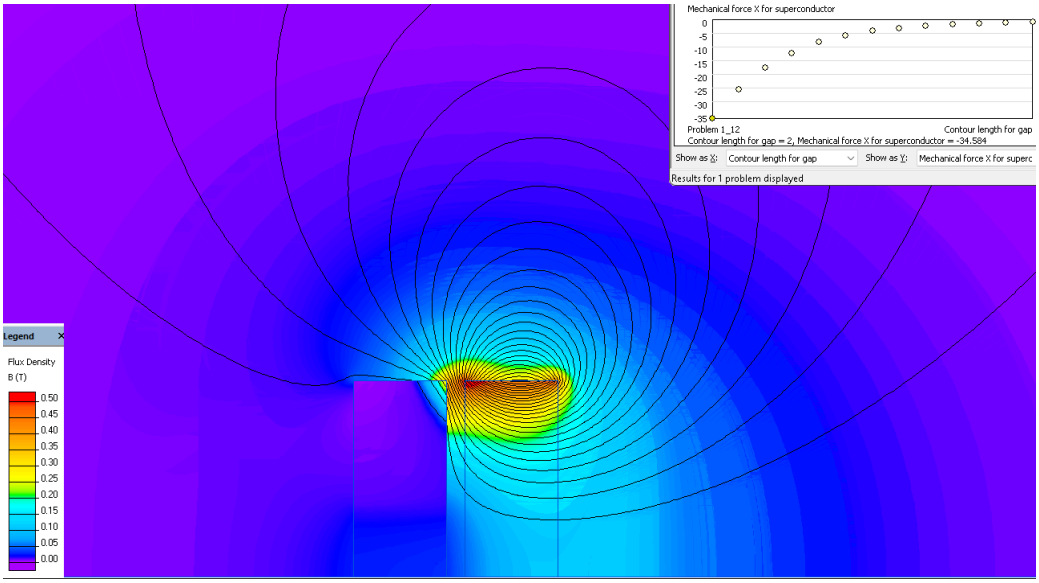

Fig 6.11: Case 1 result

CASE 2:

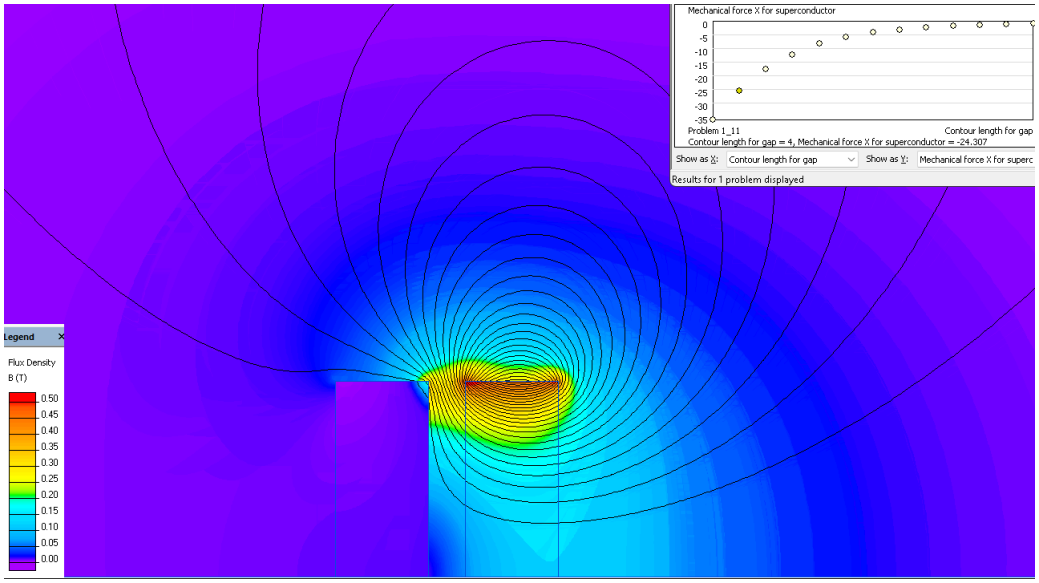

Fig 6.12: Case 2 result

CASE 3:

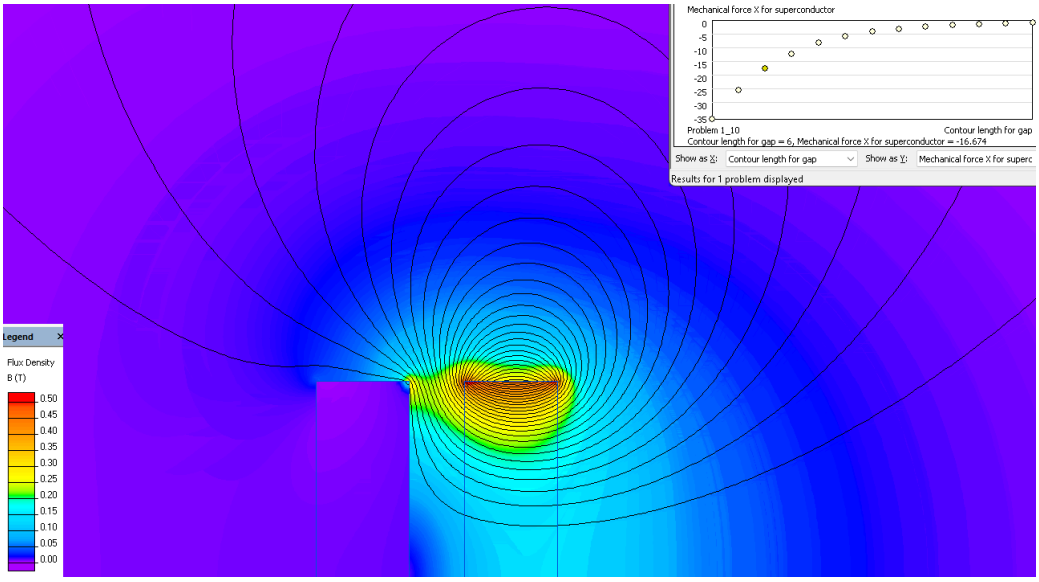

Fig 6.13: Case 3 result

CASE 4:

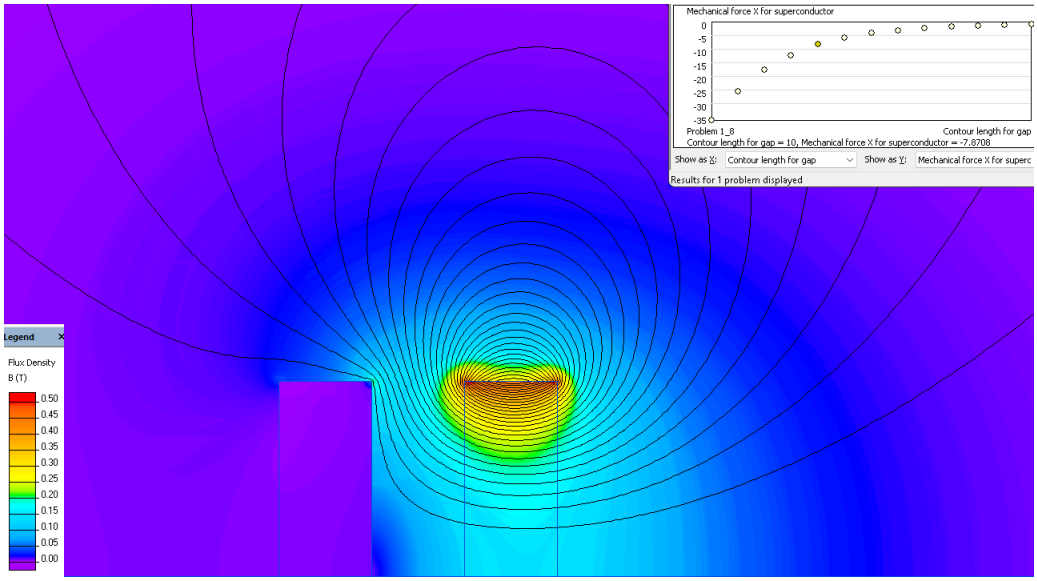

Fig 6.14: Case 4 result

CASE 5:

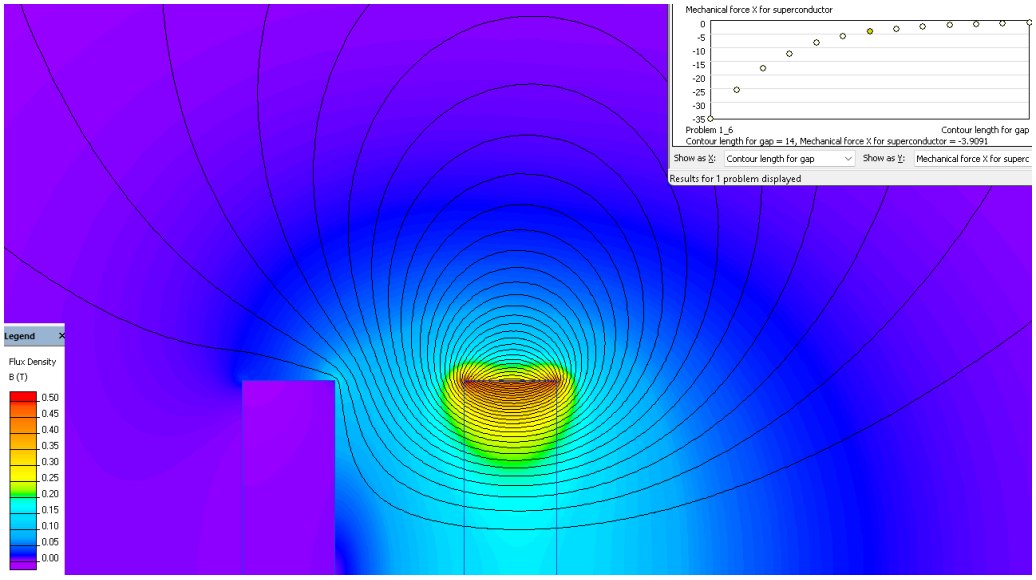

Fig 6.15: Case 5 result

CHAPTER 7: MODEL DESIGN

7.1: SOLID WORKS

History

SolidWorks Corporation was founded in December 1933 BY Massachusetts Institute of Technology graduate Jon Hirsch tick. Hirsch tick used $1 million he had made while a member of the MIT Blackjack team to set up the company. Initially based in Jon Hirsch tick United States, Hirsch tick recruited a team of engineers with the goal of building 3D CAD software that was easy-to-use, affordable, and available on the Windows desktop. Operating later from Concord Massachusetts, SolidWorks released its first product *SolidWorks 95*, in November 1995. In 1997 Dassault, best known for its CATIA CAD software, acquired SolidWorks for $310 million in stock. Jon Hirsch tick stayed on board for the next 14 years in various roles. Under his leadership, SolidWorks grew to a $100 million revenue company.

SolidWorks currently markets several versions of the SolidWorks CAD software in addition to drawings, a collaboration tool, and DraftSight, a 2D CAD product. Solid works was headed by John McAloney from 2001 to July 2007 and S Ray from 2007 to January 2011. The current CEO is Gian Paolo Basi from Jan 2015. Gian Paolo Basi replaces Bertrand Scot, who is promoted Vice President Sales of Dassault Systems Value Solutions sales channel.

SOLID WORKS is used by millions of designers and engineers at hundreds of thousands of companies. It is one of the most popular design and engineering software on the market. Known for its range of features and high functionality, SOLIDWORKS is used across multiple professions and industries around the world.

SOLIDWORKS uses parametric design, which is why it’s such an effective tool for designers and engineers. This means that the designer can see how changes will affect its neighbouring components, or even the overall solution. For example, if the size of a single component is increased, this would affect the joint or hole it’s attached to. This allows designers to spot and correct issues quickly and easily.

Solidworks features

- Simple but sophisticated 3D CAD design.
- Use templates and the CAD library for improved efficiency.
- Automation and design reuse to speed up the process.
- Cost estimation tools allow you to keep track in real-time.
- Ensure potential risks are caught early with interference check.
- Quickly produce 2D drawings for production.
- Easily create animations and photorealistic renderings.

What can Solidworks do?

As mentioned above, SOLIDWORKS is a parametric CAD program, which is easy to use and highly efficient. That makes it a favorite for both students and experienced designers. as with most software, familiarizing yourself with the buttons, names, and User Interface can take some time. However, there are some great, unique functions to aid new users in this process and optimize for the best user experience. And there are many helpful tutorials available that offer great insight and an introduction to the design process.

Rendering

Solid works Visualize allows designers to create presentation-ready, photorealistic renderings. CAD files can be opened directly in SOLIDWORKS and rendered using accurate textures, reflections, and lighting. This is a powerful feature used by most designers but is particularly useful for product designers as it allows them to demonstrate their final concept before going into production.

Solidworks simulation

SOLIDWORKS Simulation allows designers to put their designs to the test, and quickly and accurately identify any flaws. The designer will be provided with highly accurate data, which means they can make changes to the design before a physical prototype is produced. Mechanical engineers can save a lot of time, money, and effort by identifying issues with their designs early in the process.

Intricate evaluation

The Drawings tool allows a designer to quickly create 2D representations of any aspect of a design, with the option to add dimensions with the click of a button. This is useful for designers, engineers, and architects, offering the ability for a thorough evaluation.

Manufacture with ease

Once the design is complete, and the designer has eliminated potential risks identified in the simulation and evaluation, a prototype can be made. SOLIDWORKS CAM produces the design files that can be sent straight to production.

7.2: DESIGN

The landing system's design involves three essential components: a rail, the supportive framework for the rail, and a slider mechanism designed to house magnets. These magnets play a critical role in the landing process of the unmanned aerial vehicle (UAV), particularly when equipped with a superconductor.

The magnet housings are ingeniously crafted as sliders to allow for manual adjustments in the distance between two sliders. This manual alteration serves a specific purpose: it determines the rate at which the UAV decelerates during the landing phase. By modifying the spacing between these sliders, operators can precisely control and fine-tune the UAV's deceleration process.

It's important to note that the gaps created by adjusting the sliders are integral to the deceleration mechanism. Without these intentional gaps, the UAV would lack the necessary means to gradually reduce its speed during landing. The ability to manually manipulate the distance between the sliders adds a layer of flexibility and control, ensuring that the landing process can be customized to meet specific requirements and conditions. This innovative design contributes to the overall efficiency and adaptability of the UAV landing system.

There are three major parts of the design:

- Rail
- Support

- Slider

We will be discussing each part in detail in the following section:

Design of Rail:

This component holds a paramount position within the entire assembly, given its pivotal role in housing the magnets and serving as the primary landing platform for the UAV, facilitating its safe and controlled deceleration. As a housing for magnets, it ensures the precision and stability of the landing process by harnessing the magnetic forces involved. This component acts as the crucial link between the UAV and the ground, allowing the aircraft to land securely and reduce its speed efficiently. Its structural integrity and design directly impact the overall safety and effectiveness of the landing procedure, underscoring its significance as a cornerstone element in the entire system. Therefore, the intricate combination of magnet housing and landing platform characterizes it as one of the most critical and indispensable parts of the assembly, ensuring the reliable and secure operation of the UAV.

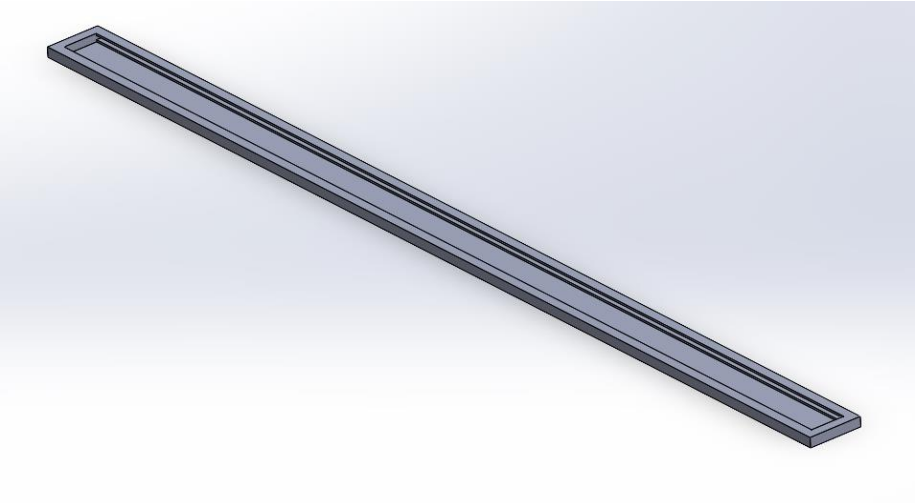

Fig 7.1: Rail Design

Design of Support:

The purpose of the support structure is fundamental in its role as a buffer against the impact loads, effectively functioning as a shield to prevent undue wear and tear. This essential component serves to absorb and distribute the force exerted, ensuring that the object or system it upholds remains resilient and

durable. By bearing the brunt of the impact, the support mitigates the potential damage or strain, thereby extending the longevity and functionality of the associated elements. In this capacity, the support plays a critical role in preserving the integrity and reliability of the overall system, making it an indispensable element in a range of applications and industries.

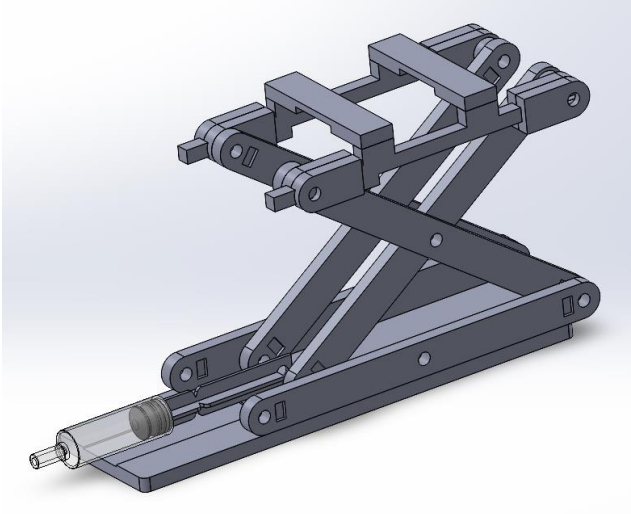

Fig 7.2: Support Design

Design of Slider:

The incorporation of the slide mechanism is to allow manual adjustment of the spacing between magnets. At the core of this concept is the idea of enhancing modularity. The ability to manually alter the distance between magnets significantly contributes to the system's flexibility and adaptability. This capability offers precise control over the deceleration process of the UAV, with the distance between magnets directly impacting the rate at which the aircraft reduces its speed during the landing phase. Therefore, the slide mechanism embodies the essence of modularity and is an essential feature for tailoring the system's performance to specific operational needs, ensuring the UAV's safe landing by optimizing its deceleration.

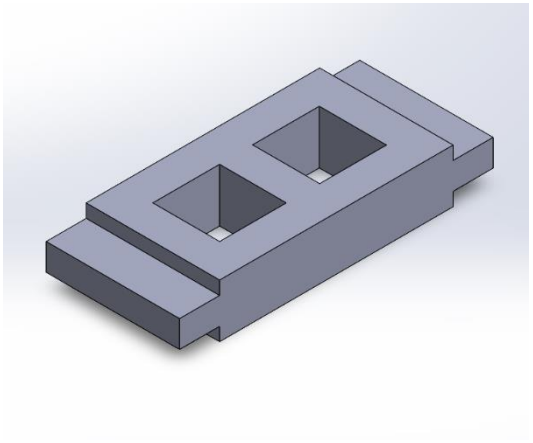

Fig 7.3: Slider Design

Assembly:

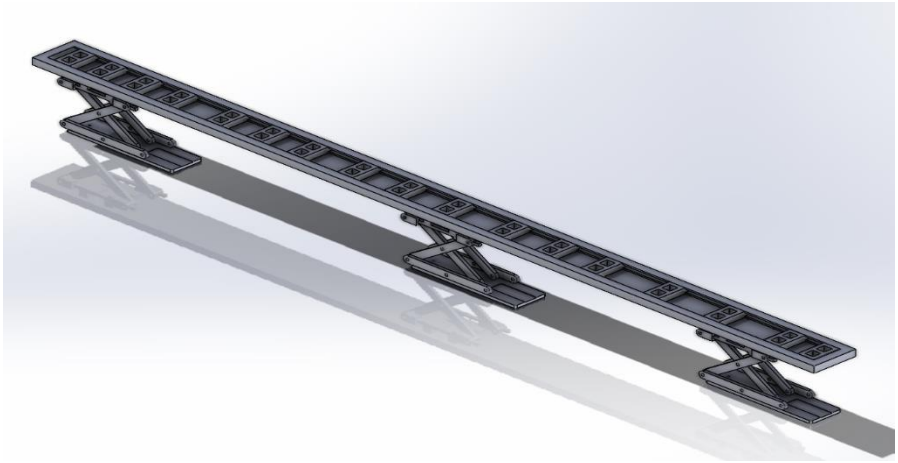

Fig 7.4: Model Design

7.3: Integration of Superconductor in UAV

The integration of a superconductor into a UAV can be achieved through a specially designed UAV base that incorporates two circular cuts. These strategically placed cuts are intended to house the superconductors and secure them flush with the base structure. This design allows for a seamless and integrated placement of the superconductors within the UAV, optimizing their functionality and impact on the overall performance of the vehicle.

The circular cuts serve a dual purpose: first, they provide a designated space to accommodate the superconductors, ensuring a secure fit within the UAV structure. Second, the flush positioning of the superconductors with the base promotes

aerodynamic efficiency, minimizing any potential disruptions to the airflow around the UAV during flight.

This design approach is not only practical but also considers the specific needs and characteristics of superconductors. By incorporating circular cuts that snugly house the superconductors, the UAV can capitalize on the unique properties of these materials, such as their ability to conduct electrical current with zero resistance and expel magnetic fields, contributing to enhanced performance and efficiency in various applications.

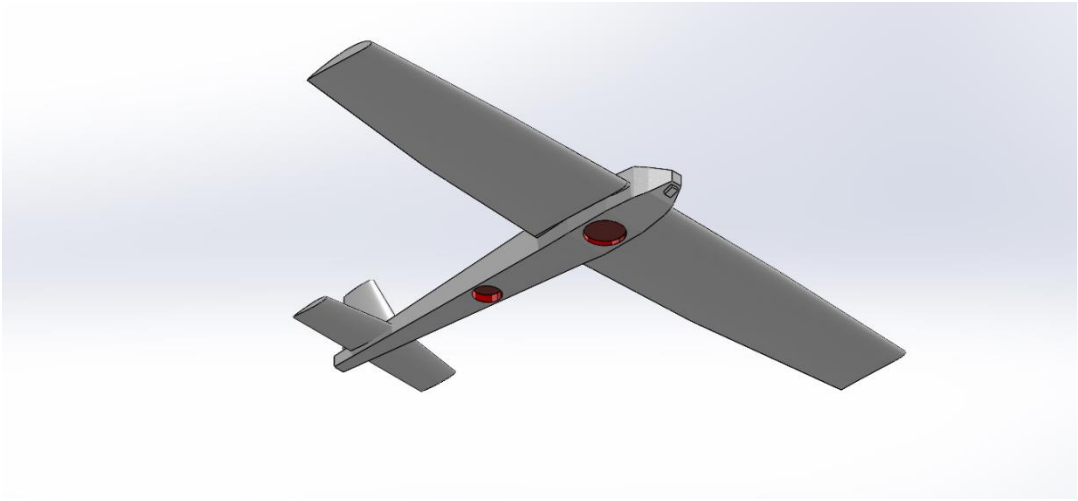

Fig 7.5: Superconductor Integration

CHAPTER 8: CONCLUSION

In summary the idea of a "UAV Landing System Using Quantum Locking Mechanism" brings together the cutting-edge quantum technology and the evolving field of aerial vehicles (UAVs). While this innovative approach is still, in its stages of development it holds promise for exciting and significant implications.

However, it's crucial to recognize that making this concept a reality depends on advancements in quantum technology and materials science. Additionally, considerations related to regulations and ethics will shape the implementation of quantum locked UAVs.

The landing system's structure will comprise a rail, the supporting structure for the rail, and a slider capable of accommodating magnets. These housings for the magnets are constructed as sliders to enable the manual adjustment of the distance between two sliders. This adjustment plays a crucial role in determining the deceleration rate of the UAV, which incorporates a superconductor. Without these gaps, the UAV will not undergo the necessary slowing down process.

Key Findings:

- The YBCO crystal emerges as the most suitable superconductor for this exploration, with YBCO standing for Yttrium Barium Copper Oxide.
- The key properties for a permanent magnet in quantum locking applications are flux density and energy density. NdFeB, also known as Neodymium magnet, exhibits the highest flux density and energy density.
- The Flux Density of the magnet at the position of superconductor was determined to be 256.46 Gauss.

This mechanism can greatly benefit from future material breakthroughs. Recently, a new material known as LK-99 has been invented, representing a significant leap in materials science and offering ground-breaking properties. One of the most remarkable features of LK-99 is its promise of achieving room temperature superconductivity.

This development marks a major milestone in materials science and has transformative implications for various industries, including the field of unmanned aerial vehicles (UAVs).

Traditionally, the use of superconductors in UAVs has been hampered by the need for cryogenic cooling systems to maintain the critical temperature required for superconductivity. These cooling systems are not only bulky and complex but also energy-intensive, limiting the practicality of their application in UAVs. However, with the advent of LK-99, this limitation is effectively resolved.

Incorporating LK-99 into the construction of UAVs represents a promising direction for the aerospace industry, where efficiency, reliability, and adaptability are of paramount importance. This material breakthrough opens up new possibilities for the development of advanced UAV technology, with implications reaching far beyond the realm of unmanned aerial vehicles. It underscores the profound impact that materials science can have on shaping the future of technology and industry."

REFERENCES

[1] Sujay Jaiaraman and Madhu.S "A research review on magnetic levitation trains", ISSN 0973-4562 Vol. 10 No.33 (2015).

[2] Sukbae Lee, Ji-Hoon Kim and Young-Wan Kwon"The First Room-Temperature Ambient-Pressure Superconductor", p-ISSN 1225-1429 (2023).

[3] Taha H.Ababou "Evolution of transportation systems with quantum levitation", (2019).

[4] Shwethasingh and Aradhanasingh“Magnetic Levitation Methods and Modeling in Maglev Trains”, ISSN: 2277 128 (2014).

[5] O. Romero-Isart, L. Clemente, C. Navau, A. Sanchez, and J. I. Cirac "Quantum Magnetomechanics with Levitating Superconducting Microspheres", Phys. Rev. Lett. 109, 147205 (2012).

[6] I. V. Aleksandrova, E. L. Koshelev, A. I. Nikitenko, T. P. Timasheva & E. R. Koresheva"Magnetic Acceleration of the Levitating Sabot Made of Type-II Superconductors".

[7] D. Dew-Hughes, "Flux pinning mechanisms in type ii superconductors", Philosophical Magazine, vol. 30, no. 2, pp. 293-305 (1974).

[8] I. V. Aleksandrova, E. R. Koresheva and E. L. Koshelev "A high-pinning-Type-II superconducting maglev for ICF target delivery: main principles, material options and demonstration models".

[9] D. D. Boyd, "Causes and risk factors for fatal accidents in noncommercial twin engine piston general aviation aircraft", Accident Analysis & Prevention, vol. 77, pp. 113-119 (2015)

[10] K. Falkowski and K. Sibilski, "Magnetic levitation system for takeoff and landing airplane-project gabriel", Proceedings of the 2013 CONSOL Conference in Rotterdam, (2013).

[11] Z. Sheng and A. Hermann, "Superconductivity in the rare-earth-free tl-ba-cu-o system above liquid-nitrogen temperature", Nature, vol. 332, no. 6159, pp. 55, (1988).